



This discussion paper is/has been under review for the journal Atmospheric Measurement Techniques (AMT). Please refer to the corresponding final paper in AMT if available.

# Measuring variations of $\delta^{18}\text{O}$ and $\delta^2\text{H}$ in atmospheric water vapour using laser spectroscopy: an instrument characterisation study

F. Aemisegger<sup>1</sup>, P. Sturm<sup>2,3</sup>, P. Graf<sup>1</sup>, H. Sodemann<sup>1</sup>, S. Pfahl<sup>1</sup>, A. Knohl<sup>2,4</sup>, and H. Wernli<sup>1</sup>

<sup>1</sup>Institute for Atmospheric and Climate Sciences, ETH Zurich, Switzerland

<sup>2</sup>Institute of Agricultural Sciences, ETH Zurich, Switzerland

<sup>3</sup>Empa, Swiss Federal Laboratories for Materials Science and Technology, Laboratory for Air Pollution and Environmental Technology, Dübendorf, Switzerland

<sup>4</sup>Faculty of Forest Sciences and Forest Ecology – Bioclimatology, Georg-August University of Göttingen, Germany

Received: 25 January 2012 – Accepted: 2 February 2012 – Published: 15 February 2012

Correspondence to: F. Aemisegger (franziska.aemisegger@env.ethz.ch)

Published by Copernicus Publications on behalf of the European Geosciences Union.

AMTD

5, 1597–1655, 2012

Characterisation of water vapour isotope measurements by laser spectroscopy

F. Aemisegger et al.

Title Page

Abstract

Introduction

Conclusions

References

Tables

Figures

◀

▶

◀

▶

Back

Close

Full Screen / Esc

Printer-friendly Version

Interactive Discussion



## Abstract

Variations of stable water isotopes in water vapour have become measurable at a measurement frequency of about 1 Hz in recent years using novel laser spectroscopic techniques. This enables us to perform continuous measurements for process-based investigations of the atmospheric water cycle at the time scales relevant for synoptic meteorology. An important prerequisite for the interpretation of data from automated field measurements lasting for several weeks or months is a detailed knowledge about instrument properties and the sources of measurement uncertainty. We present here a comprehensive characterisation and comparison study of two commercial laser spectroscopic systems based on cavity ring-down spectroscopy (Picarro) and off-axis integrated cavity output spectroscopy (Los Gatos Research). The uncertainty components of the measurements were first assessed in laboratory experiments, focussing on the effects of (i) water vapour mixing ratio, (ii) measurement stability, (iii) uncertainties due to calibration and (iv) response times of the isotope measurements due to adsorption-desorption processes on the tubing and measurement cavity walls. Based on the experience from our laboratory experiments we set up a one-week field campaign for comparing measurements of the ambient isotope signals of the two laser spectroscopic systems. The optimal calibration strategy determined for both instruments was applied as well as the correction functions for water vapour mixing ratio effects. The root mean square difference between the isotope signals from the two instruments during the field deployment was 2.3‰ for  $\delta^2\text{H}$ , 0.5‰ for  $\delta^{18}\text{O}$  and 3.1‰ for deuterium excess. These uncertainty estimates from field measurements compare well to those found in the laboratory experiments. The present quality of measurements from laser spectroscopic instruments combined with a calibration system opens new possibilities for investigating the atmospheric water cycle and the land-atmosphere moisture fluxes.

AMTD

5, 1597–1655, 2012

## Characterisation of water vapour isotope measurements by laser spectroscopy

F. Aemisegger et al.

[Title Page](#)

[Abstract](#)

[Introduction](#)

[Conclusions](#)

[References](#)

[Tables](#)

[Figures](#)

◀

▶

[Back](#)

[Close](#)

[Full Screen / Esc](#)

[Printer-friendly Version](#)

[Interactive Discussion](#)



# 1 Introduction

The atmospheric transport patterns of water vapour significantly influence local climates and Earth's surface hydrology. As naturally available tracers of phase transitions of water, stable isotopes provide useful information on the atmospheric water cycle, in particular on conditions during phase changes such as evaporation from the sea surface (Pfahl and Wernli, 2008; Sodemann et al., 2008; Uemura et al., 2008), plant transpiration (Farquhar et al., 2007), cloud formation (Federer et al., 1982; Ciais and Jouzel, 1994) and post-condensation exchange with below cloud vapour (Field et al., 2010). To investigate these processes and their impact on stable water isotopes in atmospheric waters at the temporal scale of significant weather events high frequency measurements of stable water isotopes are essential. Such measurements can also help to validate model parametrisations of evaporation (He and Smith, 1999), transpiration (Dongmann et al., 1974) and rainfall re-evaporation (Lee and Fung, 2008).

Stable water isotope measurements in liquid waters have been used for several decades as a means to probe the hydrologic cycle and to gain insight into its fundamental processes (Gat, 1996). The international atomic energy agency (IAEA) and the World Meteorological Organisation (WMO) have been surveying the content of hydrogen and oxygen isotopes in precipitation since 1961 in the framework of their Global Network on Isotopes in Precipitation (GNIP; Araguas et al., 1996). The key mechanisms influencing the abundance of heavy water isotopes in meteoric waters on relatively long, typically monthly timescale have subsequently been identified (Craig, 1961; Dansgaard, 1964; Gat and Dansgaard, 1972). The dependency of the isotopic composition of precipitation on meteorological conditions during phase changes has been used for inferring information about past climate from paleo-archives (Dansgaard et al., 1993; Jouzel et al., 1997; Johnsen et al., 2001).

Stable isotopes have been less extensively measured in water vapour than in the liquid phase, mainly because such measurements have been very laborious and error-prone until recently (Helliker and Noone, 2010), involving cryogenic trapping with

[Title Page](#)

[Abstract](#)

[Introduction](#)

[Conclusions](#)

[References](#)

[Tables](#)

[Figures](#)

◀

▶

[Back](#)

[Close](#)

[Full Screen / Esc](#)

[Printer-friendly Version](#)

[Interactive Discussion](#)

**Characterisation of water vapour isotope measurements by laser spectroscopy**

F. Aemisegger et al.

[Title Page](#)[Abstract](#)[Introduction](#)[Conclusions](#)[References](#)[Tables](#)[Figures](#)[◀](#)[▶](#)[◀](#)[▶](#)[Back](#)[Close](#)[Full Screen / Esc](#)[Printer-friendly Version](#)[Interactive Discussion](#)

Here, we present results from a characterisation and inter-comparison study of two commercial laser spectroscopic instruments for high frequency measurements of the three stable water isotopes  $^1\text{H}_2^{16}\text{O}$ ,  $^1\text{H}_2^{18}\text{O}$  and  $^2\text{H}^1\text{H}_2^{16}\text{O}$  in water vapour. Our primary aim is to provide a complete uncertainty assessment for the Picarro L1115-i system. A second laser spectroscopic instrument, the WVIA by Los Gatos Research, which was extensively characterised by Sturm and Knohl (2010) is used for comparison in a slightly modified setup (improved temperature stabilisation and slightly different water vapour mixing ratio dependency). The two latest versions (L2130-i and WVIA-EP) of both systems were tested as well and our findings with respect to improvements will be discussed. The proposed assessment considers four important aspects: (1) an inter-comparison of measurement quality between the two analysers and with IRMS is done using 12 liquid standards, (2) the water vapour mixing ratio dependencies of isotope measurements are quantified, (3) the stability of the systems in terms of precision as well as in terms of optimal calibration frequency is investigated, and (4) the response times of the measurement systems after a step change in isotope and water concentration are characterised. The structure of this paper follows the description and evaluation of these 4 characterisation steps. At the end a short case study is presented of comparative ambient air measurements in field conditions with the two laser systems operated in a way that was found optimal during the laboratory tests.

## 20 2 Instrumentation

### 2.1 Quantification of the isotopic content of water samples

The heavy isotopic content of a given water vapour sample is generally expressed in terms of permil deviation of the isotopic mixing ratio from an internationally approved standard:

$$25 \quad \delta = \frac{R_{\text{sample}} - R_{\text{standard}}}{R_{\text{standard}}}, \quad (1)$$

## Characterisation of water vapour isotope measurements by laser spectroscopy

F. Aemisegger et al.

[Title Page](#)

[Abstract](#)

[Introduction](#)

[Conclusions](#)

[References](#)

[Tables](#)

[Figures](#)

◀

▶

[Back](#)

[Close](#)

[Full Screen / Esc](#)

[Printer-friendly Version](#)

[Interactive Discussion](#)

where  $R$  represents the ratio of the rare, heavy isotopic concentration ( ${}^2\text{H}{}^1\text{H}{}^{16}\text{O}$  or  ${}^1\text{H}_2{}^{18}\text{O}$ ) to the concentration of the most abundant, lighter species ( ${}^1\text{H}_2{}^{16}\text{O}$ ). The  $\delta$  values are generally indicated in permil. The international reference standard  $R_{\text{standard}}$  is known as the Vienna Standard Mean Ocean Water (VSMOW; Gonfiantini, 1978) distributed by the IAEA. When measuring isotopic composition of water samples, the delta values have to be normalised according to the IAEA VSMOW2-SLAP2 scale as described in IAEA (2009), which corresponds to a two point calibration with a fixed zero point (VSMOW) and a normalisation factor (SLAP, Standard Light Antarctic Precipitation).

## 10 2.2 Laser spectroscopic measurements of stable water isotopes in water vapour

Two physically different measurement principles allow to quantify the isotopic composition of natural waters. Atomic mass spectrometric analysis takes advantage of the differing mass-to-charge ratio of isotopes. Laser spectroscopic systems use the difference in excitation energy levels of isotopes, leading to a characteristic absorption behaviour of the molecules when exposed to electromagnetic radiation. Three nearby absorption peaks in the infrared corresponding to the three molecules  ${}^2\text{H}{}^1\text{H}{}^{16}\text{O}$ ,  ${}^1\text{H}_2{}^{18}\text{O}$ , and  ${}^1\text{H}_2{}^{16}\text{O}$  are scanned by a laser in continuous wave operation mode. The spectral regions scanned in the two instruments is different (Table 1).

20 In this work, laser spectrometric isotope and water vapour mixing ratio measurements were performed using two different types of commercial instruments. The Picarro L1115-i (older version) and L2130-i (latest version) isotopic water vapour analysers (Picarro Inc., Sunnyvale, CA, USA) are based on cavity ring-down spectroscopy (Crosson, 2008). The second type of laser systems, the water vapour isotope analysers (WVIA and WVIA-EP, DLT-100, version March 2011) by Los Gatos Research Inc. (LGR, Mountain View, CA, USA) were used as a benchmark. The WVIA and the WVIA-EP are based on off-axis integrated cavity output spectroscopy (Baer et al.,

[Title Page](#)[Abstract](#)[Introduction](#)[Conclusions](#)[References](#)[Tables](#)[Figures](#)[◀](#)[▶](#)[Back](#)[Close](#)[Full Screen / Esc](#)[Printer-friendly Version](#)[Interactive Discussion](#)

**Characterisation of water vapour isotope measurements by laser spectroscopy**

F. Aemisegger et al.

[Title Page](#)[Abstract](#)[Introduction](#)[Conclusions](#)[References](#)[Tables](#)[Figures](#)[◀](#)[▶](#)[Back](#)[Close](#)[Full Screen / Esc](#)[Printer-friendly Version](#)[Interactive Discussion](#)

acquisition rate is higher (1 Hz) compared to 0.5 Hz for L1115-i. The WVIA-EP has an improved internal temperature stability.

## 2.3 Calibration systems

Systematic errors in laser isotope ratio measurements result from drifts due to variations of environmental parameters such as temperature and pressure. In order to correct for such effects and to normalise the isotope measurements with respect to the international reference VSMOW2-SLAP2 scale, the instruments have to be calibrated at regular intervals. Parallel vapour collection in flasks and subsequent reference measurement with IRMS to calibrate the laser instrument is an option suggested by Johnson et al. (2011). However the normalisation with respect to the international reference scale is indirect in this case and biases introduced by the flask sampling may affect the measurement quality. Direct calibration involves the measurement of a standard vapour sample with known isotopic composition. Calibration standards are generally liquid water standards. Primary international standards are available from IAEA and referenced working standards are used in the different laboratories worldwide. Direct calibration of a vapour isotope analyser thus involves evaporation of these liquid standards and mixing with a carrier gas before introducing them into the optical cavity for an absorption measurement.

Liquid autosamplers as used for liquid isotopic laser analyses (Lis et al., 2008) are not optimal for calibrating vapour instruments as the produced calibration vapour quantity is very limited, making extended calibration runs of more than 5 min impracticable. Fractionation effects have to be accounted for if partial evaporation methods are used (Wen et al., 2008; Wang et al., 2009). For example, with a dew point generator as a calibration system, dry air is bubbled through a water reservoir at a specified temperature and the liquid water is continuously enriched in heavy isotopes, following a Rayleigh distillation process. The isotopic composition of the vapour can be determined if the initial and the residual water isotopic composition are known and if the temperature and pressure conditions in the water reservoir are precisely regulated. Calibration

[Title Page](#)

[Abstract](#)

[Introduction](#)

[Conclusions](#)

[References](#)

[Tables](#)

[Figures](#)

◀

▶

[Back](#)

[Close](#)

[Full Screen / Esc](#)

[Printer-friendly Version](#)

[Interactive Discussion](#)

**Characterisation of water vapour isotope measurements by laser spectroscopy**

F. Aemisegger et al.

techniques allowing complete evaporation of the liquid standards operate by continuously dripping liquid droplets into a dry air stream using a syringe pump or a capillary dripping system as proposed by Iannone et al. (2009) and used in a slightly altered setup by Sturm and Knohl (2010). Similar techniques are used in the commercial calibration systems for online water vapour isotope measurements from Picarro and Los Gatos, which have become available recently and are used in this study.

The commercial calibration system for the L1115-i instrument comprises a vaporiser and a standard delivery module A0101 (SDM; see Fig. 1a). This calibration system allows for the automated use of two liquid standards in parallel (Std1, Std2 in Fig. 1a). The standards are filled into collapsible bags (B1, B2). The liquid standards are then pumped by syringe pumps (SP1, SP2) via capillary lines (C1, C2) to the injection head (H) of the vaporiser. The injection system consists of two needle ports (P1, P2) and a carrier gas inlet (A). The head of the needles penetrates the vaporisation chamber (C), the temperature of which is regulated at 140 °C to ensure immediate and full evaporation of the liquid standard droplets introduced through the needles. The needle port is sealed with three o-rings (R) to avoid ambient air penetration into the vaporisation chamber when no calibration is done, and to prevent leaking of dry air during calibration. When a calibration run is performed, the liquid standards are pumped drop-wise into the vaporiser and a constant dry air flow sustains immediate evaporation of the liquid droplets in the air stream. The dry air, serving as a carrier gas is pumped at a rate of 200 ml min<sup>-1</sup> through a molecular sieve 5A MT-D 200 cm<sup>3</sup> (D) with Drierite indicator (Agilent) into the vaporiser. Alternatively, dry synthetic air (Alphagas synthetic air, Carbagas, H<sub>2</sub>O < 3 µmol mol<sup>-1</sup>, C<sub>n</sub>H<sub>m</sub> < 0.5 µmol mol<sup>-1</sup>, O<sub>2</sub> = 20 % ± 1 %) was used at an over-pressure of 0.4 bar (DA) (see Sect. 3.3), while the dry air pump was switched off. The waste port valve (W) of the vaporiser is constantly opened in order to establish a steady flow through the vaporising chamber. To exclude memory effects from the previous calibration run and to allow the moist air equilibrium in the vaporiser to be reached, the outlet valve (V) of the vaporiser to the measurement cell is switched open only after a delay of five minutes. The water vapour mixing ratio of the calibration gas

[Title Page](#)[Abstract](#)[Introduction](#)[Conclusions](#)[References](#)[Tables](#)[Figures](#)[◀](#)[▶](#)[Back](#)[Close](#)[Full Screen / Esc](#)[Printer-friendly Version](#)[Interactive Discussion](#)

can be varied in the range 2000–30 000 ppmv by controlling the liquid pumping rate between 0.005  $\mu\text{l s}^{-1}$  and 0.08  $\mu\text{l s}^{-1}$ .

The central element of the water vapour isotope standard source (WVISS, Fig. 1b) by Los Gatos Research is a nebulising system (N) guiding a capillary inlet line (L), which serves as a dripping system into a 1 l spray chamber (S) heated to 80 °C. Ambient air is pumped through a two stage drying system (D) containing a regenerative desiccant air dryer and a replaceable Drierite cartridge. The water vapour mixing ratio can be regulated via a mass flow controller (MFC), which adjusts the dry air flow rate (0–10  $\text{l min}^{-1}$ ). This way water vapour mixing ratios in the range 5000–30 000 ppmv can be produced. A three way solenoid valve (SV) controls the vapour source, which is either the calibration vapour (CV) or ambient air (AA). The system allows only for one automated liquid standard (Std) to be measured when calibration is unattended. In addition to producing only one vapour standard, the disadvantage of the LGR calibration system is its bulkiness (Table 1), which complicates field work. However, in contrast to the Picarro system, it allows for stable production of large quantities of calibration vapour over several days.

### 3 Experiments

#### 3.1 Delta scale linearity experiment

The focus of this first experiment was to verify the linearity of the calibrated laser spectroscopic measurements in the VSMOW2-SLAP2 range of the isotope delta scale with an independent measurement technique. Ten working standards (WS 1–10, Table 2) were measured with both laser instruments and the WVISS calibration unit for 10 min each at a water vapour mixing ratio of 18 000 ppmv. The first two minutes and the last minute of each calibration run were discarded. All measurements were done twice (run 1 and run 2), each time over a continuous 8 h time period. Furthermore, between two working standard calibration runs we measured a drift standard for three minutes in order to remove memory effects from the calibration unit.

[Title Page](#)

[Abstract](#)

[Introduction](#)

[Conclusions](#)

[References](#)

[Tables](#)

[Figures](#)

◀

▶

◀

▶

[Back](#)

[Close](#)

[Full Screen / Esc](#)

[Printer-friendly Version](#)

[Interactive Discussion](#)

The standards measured with the two laser spectrometers were compared to IRMS measurements, done on a Delta<sup>PLUS</sup>XP mass spectrometer (Thermo Fisher Scientific Inc., Germany) using a high-temperature conversion/elemental analyser coupled online to the mass spectrometer via a ConFlo III interface (Gehre et al., 2004).

Both measurements using IRMS and laser spectroscopy were calibrated and normalised to the VSMOW2-SLAP2 scale (IAEA, 2009). For the calibration and normalisation of IRMS measurements, WS 11 and WS 12 were used. For the calibration of laser spectroscopic measurements the IAEA standards VSMOW2 and SLAP2 were used directly.

## 10 3.2 Water vapour mixing ratio calibration

For the investigation of the water vapour concentration dependency of isotope measurements the water vapour mixing ratio data of the two instruments had to be calibrated. A dew point generator (LI-610, LI-COR Inc., Lincoln, NE, USA) was used for this purpose. Two water vapour mixing ratio calibration series were performed. In 15 one of these two runs both instruments were connected in parallel to the dew point generator and measured water vapour mixing ratios simultaneously from the same source. Another run was performed with only the L1115-i instrument connected to the LI-610. Mixing ratios between 3000 and 30 000 ppmv were produced in a constant flow of  $1\text{ l min}^{-1}$  of moist air with an uncertainty of  $\sim 100\text{--}400\text{ ppmv}$  (increasing for larger dew point temperatures). Calibration runs always lasted for at least 2 h for each dew point temperature; 1 h for equilibration of the air flow through the water reservoir in the dew point generator and 1 h of measurements considered in the data analysis. The calibration functions determined from the laboratory experiments were then used in order 20 to calibrate the data of each instrument. To verify the parallel water vapour mixing ratio calibration experiment from the laboratory, ambient measurements of water vapour mixing ratio were performed in parallel in a field setup as described in Sect. 3.6.

[Title Page](#)[Abstract](#)[Introduction](#)[Conclusions](#)[References](#)[Tables](#)[Figures](#)[◀](#)[▶](#)[◀](#)[▶](#)[Back](#)[Close](#)[Full Screen / Esc](#)[Printer-friendly Version](#)[Interactive Discussion](#)

### 3.3 Water concentration dependency experiment

The calibration unit by Picarro was used for investigating the water concentration dependency of the L1115-i laser instrument. Four calibration runs were performed in steps of 1000 ppmv in the range 2000–30 000 ppmv using four different standards (WS 6–9, Table 2). Calibration runs lasted for 20 min each. Depending on the type of carrier gas used, interfering effects can affect the calibration gas measurements. For example remaining ambient water vapour, when using dry cells can change the isotopic values of the standard. Furthermore, traces of other gases also absorbing laser light in the same spectral domain can affect the measurements. To investigate the effect of the carrier gas source, two different carrier gases were compared: (1) synthetic dry air from a gas cylinder and (2) dried ambient air using a molecular sieve with indicating Drierite (Sect. 2.3). The calibration runs for each standard were done twice in blocks of approximately one day. The carrier gas sources were alternated. The data was calibrated independently using the WVISS calibration unit and the IAEA standards VSMOW2 and SLAP2 at a water vapour mixing ratio of 18 000 ppmv.

The concentration dependency of the L2130-i was tested using the WVISS with dry ambient air as a carrier gas. Only WS 6 was used for testing this instrument.

### 3.4 Water vapour isotope measurement stability experiment

The stability of the WVIA and the L1115-i were tested in terms of short-term and long-term drifts. The effect of those drifts on precision and accuracy was then investigated. The two experimental setups for these tests were identical. The two instruments were connected to the WVISS in parallel in such a way that both measured the same water vapour signal. The two latest versions of each instrument (L2130-i and WVIA-EP) were also tested in terms of short-term stability using the WVISS.

[Title Page](#)

[Abstract](#)

[Introduction](#)

[Conclusions](#)

[References](#)

[Tables](#)

[Figures](#)

◀

▶

◀

▶

[Back](#)

[Close](#)

[Full Screen / Esc](#)

[Printer-friendly Version](#)

[Interactive Discussion](#)

### 3.4.1 Short-term stability

Short-term stability was tested by measuring WS 6 (Table 2) at a water vapour mixing ratio of 15 700 ppmv over 24 h. An Allan variance analysis was then performed using the measured  $\delta^2\text{H}$  and  $\delta^{18}\text{O}$  time series in order to get a quantitative estimate of the 5 precision of the signals at different aggregation time scales.

Introduced by Allan (1966) and presented by Werle (2011) as a general method to characterise the stability of tunable diode laser absorption spectrometers, the Allan plot is a useful analysis tool of the precision and the drift components of such a measurement system over time. The Allan variance measures difference between two consecutive 10 signal values  $y_i$  and  $y_{i+1}$  at a given aggregation time scale  $\tau$  averaged over the total number of averaging intervals  $n$ :

$$\sigma_A^2(\tau) = \frac{1}{2n} \sum_{i=1}^n (y_{i+1}(\tau) - y_i(\tau))^2 \quad (2)$$

The Allan variance can be used for a measure of precision and should be computed for different averaging times. The optimum averaging time  $\tau_0$  is obtained when the Allan 15 variance as a function of averaging time reaches a minimum  $\min(\sigma_A^2(\tau))$ . The minimum Allan variance corresponds to the maximum precision that can be reached with the instrument. At averaging times  $> \tau_0$  the measurements are affected by instrument drifts, which are due to changing environmental characteristics. The precision at the highest 20 possible temporal resolution given by the instrument is important if high frequency measurements are of interest.

### 3.4.2 Long-term stability

For time scales much longer than the optimum averaging time the Allan variance analysis is not a useful assessment tool, as it only shows the evolution of the drift component. A stability analysis for time scales of several days is nevertheless interesting for

[Title Page](#)[Abstract](#)[Introduction](#)[Conclusions](#)[References](#)[Tables](#)[Figures](#)[◀](#)[▶](#)[◀](#)[▶](#)[Back](#)[Close](#)[Full Screen / Esc](#)[Printer-friendly Version](#)[Interactive Discussion](#)

finding the ideal calibration scheme. Long term stability was investigated by measuring WS 6 at regular intervals of 30 min for a duration of 10 min. During the remaining 20 min ambient air was measured. This regular calibration sequence was performed over 14 days. The first two minutes and the last minute of each calibration run were 5 discarded for the data analysis to avoid biases due to non-steady state effects. The calibration runs were then used to evaluate the optimal inter-calibration time.

### 3.5 Response time experiment

The response time of a measurement system is an important characteristic of a laser spectroscopic instrument for field measurements of stable water isotopes. It serves 10 as a design quantity for an optimal gas sampling system and determines the exact timing of the measurement. The primary aim of a good sampling system is to minimise interactions of the sample gas with the tubing material. The parameters influencing response time are the tubing material (Sturm and Knohl, 2010; Schmidt et al., 2010), temperature and length as well as pumping rate.

The response time of the measurement system can be described using two temporal 15 response components, a time lag  $\tau_{\text{lag}}$ , accounting for the retardation of the vapour sample in the tubing system and an exponential time constant  $\tau_{\text{ads}}$  determined by the exchange rate of the gas in the optical cell, the effect of adsorption and desorption from the tubing surface as well as the very slow diffusion through the tubing walls. The time lag for the sample to reach the cavity can be derived from experimental data. It 20 depends on the tubing length and the pumping rate of the individual instruments. In the setup used here  $\tau_{\text{lag}} = 88$  s for the L1115-i instrument and 75 s for the WVIA system with a 12 mm PFA sample line length of 15.5 m. In Fig. 2 the two time constants are schematically explained using an example of a response in  $\delta^2\text{H}$  measured by L1115-i. The input signal to the measurement system can be described by a step-function, 25 representing the switching of a valve between two reservoirs containing two gases with a different water vapour mixing ratio and isotopic composition. Here step changes were

<a href="#">Title Page</a>	
<a href="#">Abstract</a>	<a href="#">Introduction</a>
<a href="#">Conclusions</a>	<a href="#">References</a>
<a href="#">Tables</a>	<a href="#">Figures</a>
<a href="#">◀</a>	<a href="#">▶</a>
<a href="#">◀</a>	<a href="#">▶</a>
<a href="#">Back</a>	<a href="#">Close</a>
<a href="#">Full Screen / Esc</a>	

<a href="#">Printer-friendly Version</a>
<a href="#">Interactive Discussion</a>

done by switching between ambient laboratory water vapour and calibration vapour from the WVISS calibration unit.

The response function from the measurement system can be described approximately using the two time constants  $\tau_{\text{lag}}$  and  $\tau_{\text{ads}}$  and the concentration difference of the two samples ( $c_0, c_1$ ). The concentration  $c_0$  of the vapour before the switch is determined by averaging the data measured in the 30 s time period before the switch. The concentration after the switch is averaged from 4.5 min to 10 min after the switch (see Fig. 2, dashed lines). We use a simple model of gas exchange in a cavity assuming perfect mixing. The change in concentration as measured by the instrument after a step change in the input signal from  $c_0$  to  $c_1$  can be described as follows:

$$c(t) = c_1 + (c_0 - c_1) \exp\left(-\frac{(t - \tau_{\text{lag}})}{\tau_{\text{ads}}}\right) \quad (3)$$

This theoretical response function is fitted by least squares with quality criteria of a root mean square error of  $\text{RMSE}_{\delta^{18}\text{O}} < 2\text{\textperthousand}$ ,  $\text{RMSE}_{\delta^2\text{H}} < 10\text{\textperthousand}$ , and  $\text{RMSE}_{\text{H}_2\text{O}} < 1000 \text{ ppmv}$ . For the fitting, the data obtained during the first two minutes of the response are weighted by a factor of 10, thus ensuring that slight oscillations in the equilibrium value  $c_0$  do not affect the estimated response time  $\tau_{\text{ads}}$  substantially. The fitting procedure serves as a quality control of the switches and allows to eliminate step changes during which the calibration unit did not work properly, due to blocking of the capillary tubing or air pump problems. The exponential time constant  $\tau_{\text{ads}}$  of the response signals is calculated separately for the water vapour mixing ratio,  $\delta^{18}\text{O}$  and  $\delta^2\text{H}$ . Step changes of  $\sim 60\text{\textperthousand}$  in  $\delta^2\text{H}$  (between  $-80\text{\textperthousand}$  and  $-140\text{\textperthousand}$ ),  $\sim 7\text{\textperthousand}$  in  $\delta^{18}\text{O}$  (between  $-25\text{\textperthousand}$  and  $-32\text{\textperthousand}$ ) and  $\sim 10\,000 \text{ ppmv}$  in  $\text{H}_2\text{O}$  (between 12 000 ppmv and 22 000 ppmv) were performed for external tubing temperatures of 30 °C (18 steps), 60 °C (48 steps), 90 °C (38 steps) and 120 °C (8 steps). The temperature of the heated tubing (Lohmann Wärmetechnik und Regelung, Graz) was regulated at the splitting end between L1115-i and WVISS using a R1140 regulator (elotech, Germany) with a SIRIUS SC semiconductor contactor (Siemens, Germany).

[Title Page](#)[Abstract](#)[Introduction](#)[Conclusions](#)[References](#)[Tables](#)[Figures](#)[◀](#)[▶](#)[Back](#)[Close](#)[Full Screen / Esc](#)[Printer-friendly Version](#)[Interactive Discussion](#)

In our experimental setup a step towards lower water vapour mixing ratios always corresponds to a step towards more depleted isotope values, which implies that both water and isotope fluxes between the wall and the bulk gas in the tubing have the same direction. During a step change from high to low water and isotope concentration

5 (switch down) water molecules desorb from the tubing and cavity walls. A step change towards higher water and isotope concentration implies adsorption of water molecules on the tubing and cavity material. In this experiment the external tubing effects were the same for both instruments. Internal memory effects induced by adsorption on tubing and the cavity wall of the instruments were however different.

## 10 3.6 Comparative ambient air measurements

Ambient air measurements were performed on the roof of a tower building in Zurich (47.38°, 8.55°, ~ 500 m a.s.l.) in the period 19–26 July 2011 with both L1115-i and WVIA connected to the same inlet. The L1115-i was setup in a dedicated box outside with a short stainless steel sampling line of 70 cm length with an outer diameter of 1/8 inch. The WVIA was setup in a room and a 23 m long PTFE sampling line with an outer diameter of 1/4 inch was used.

Throughout the remainder of this paper, red color coding for WVIA and WVIA-EP measurements and blue color coding for L1115-i and L2130-i measurements is used in the figures, except if explicitly mentioned.

## 20 4 Results and discussion

## 4.1 Delta scale linearity

In the calibration experiment ten laboratory working standards of stable water isotopes were measured and calibrated with the two laser systems as well as with IRMS. All calibrated laser spectroscopy measurements are in very good agreement with the calibrated IRMS values ( $R^2 > 0.99$  for both isotopes). We found a small isotope ratio

---

**Characterisation of water vapour isotope measurements by laser spectroscopy**

F. Aemisegger et al.

[Title Page](#)[Abstract](#)[Introduction](#)[Conclusions](#)[References](#)[Tables](#)[Figures](#)[◀](#)[▶](#)[Back](#)[Close](#)[Full Screen / Esc](#)[Printer-friendly Version](#)[Interactive Discussion](#)

of these runs is 0.7‰ for  $\delta^2\text{H}$  and 0.3‰ for  $\delta^{18}\text{O}$  for both instruments. These values are in the order of the uncertainties quantified in Table 3.

For the ten samples measured here, the average standard deviation of the IRMS measurements is  $\sigma(\delta^2\text{H}) = 0.9\text{‰}$  and  $\sigma(\delta^{18}\text{O}) = 0.4\text{‰}$  (Table 3). These values do not include any sampling uncertainty (e.g. cryogenic trapping of a water vapour sample for later analysis). The laser spectroscopic measurements however include sampling uncertainties in this experimental setup and show comparable values (except for the higher  $\delta^2\text{H}$  uncertainty in L1115-i).

The uncertainties of the isotope standard measurements with the two laser spectroscopic systems are dependent on the  $\delta$  value of the standards and become higher with increasing depletion of the standards' isotopic composition (Fig. 4). The larger uncertainties of L1115-i standard measurements (blue crosses) compared to WVIA (red crosses) are due to the lower short-term precision of the instrument (Sect. 4.4.1 below) and to the longer response time characteristics (Sect. 4.5 below), which introduce larger memory effects than for WVIA.

An important aspect of the calibration strategy of a laser spectroscopic instrument is whether a two point calibration is necessary or if a one point calibration (only bias correction) is sufficient. The calibration system WVISS only allows for automatic measurements using one standard. To investigate this aspect we computed the normalisation factors and their uncertainty following IAEA (2009) for the two calibration runs (Table 4). For L1115-i the normalisation factors as well as the intercepts were different in the two runs. For WVIA we found that the normalisation factors remained within the uncertainty range, the intercept however changed. This might indicate that regular two point calibration is necessary for L1115-i and that one standard might be sufficient for WVIA calibration, but further investigation with more calibration runs would be needed to confirm this preliminary finding.

[Title Page](#)[Abstract](#)[Introduction](#)[Conclusions](#)[References](#)[Tables](#)[Figures](#)[◀](#)[▶](#)[Back](#)[Close](#)[Full Screen / Esc](#)[Printer-friendly Version](#)[Interactive Discussion](#)

## 4.2 Water vapour mixing ratio calibration

AMTD

5, 1597–1655, 2012

### Characterisation of water vapour isotope measurements by laser spectroscopy

F. Aemisegger et al.

The measurement range of the water vapour mixing ratio specified by the two manufacturers is between 5000 and 30 000 ppmv, which was well covered by our water vapour mixing ratio calibration measurements. The water vapour mixing ratios measured by the L1115-i and the WVIA instruments both show a linear relationship with the theoretical dew point generator values over the whole measurement range as can be seen from the calibration line of L1115-i in Fig. 5a and the grey line in Fig. 5b, which illustrates the correspondence of the L1115-i and the WVIA values. The calibration lines obtained here for water vapour mixing ratio for the two instruments are the following:

$$H_2O_{L1115-i,cal} = 0.79 \cdot H_2O_{L1115-i,m} + 318 \text{ ppmv} \quad (4)$$

$$H_2O_{WVIA,cal} = 0.92 \cdot H_2O_{WVIA,m} + 117 \text{ ppmv} \quad (5)$$

The water vapour mixing ratio calibration procedure using a dew point generator is time consuming and lasts for several days due to the long equilibration and measurement times. It can thus not be repeated regularly without a major loss of ambient measurement time. The error associated with using the same calibration parameters for the water vapour mixing ratio during a measurement campaign can be quantified by the standard error of the calibration fitting in Fig. 5a, for which data from two independent calibration runs (full circles and white squares) were used. The water vapour mixing ratio uncertainty resulting from the calibration parameters thus amounts to  $\sim 400$  ppmv. Compared to the parallel laboratory run with the dew point generator (white squares and grey line in Fig. 5b), the parallel field run (blue line in Fig. 5b) shows a larger spread (85 ppmv standard error for the field measurements vs. 20 ppmv standard error for the lab measurements) and a bias ( $\sim 1300$  ppmv) with respect to the laboratory correspondence line. This indicates that the measurement uncertainty in field measurements is higher than what could be quantified under controlled conditions in the laboratory. Effects from the sampling lines (material and length) may play a role in this higher uncertainty. The bias with respect to the laboratory correspondence line indicates a need

<a href="#">Title Page</a>	
<a href="#">Abstract</a>	<a href="#">Introduction</a>
<a href="#">Conclusions</a>	<a href="#">References</a>
<a href="#">Tables</a>	<a href="#">Figures</a>
<a href="#">◀</a>	<a href="#">▶</a>
<a href="#">◀</a>	<a href="#">▶</a>
<a href="#">Back</a>	<a href="#">Close</a>
<a href="#">Full Screen / Esc</a>	
<a href="#">Printer-friendly Version</a>	
<a href="#">Interactive Discussion</a>	

for more frequent water vapour mixing ratio calibration than just sporadic laboratory calibrations if accurate water vapour mixing ratios are required.

For the remainder of this study, we adopted the calibration lines obtained from the laboratory calibration run to correct water vapour mixing ratios and used results from the parallel field run as an uncertainty estimate.

### 4.3 Dependency of the isotope measurement on water vapour mixing ratio

The spectroscopic measurements of water vapour isotopes are affected by water vapour mixing ratio in two ways. First, the precision of the measurement depends on the water vapour mixing ratio. Second, the isotope measurement is affected by a bias, which depends on water vapour mixing ratio. Both aspects were already covered by Sturm and Knohl (2010) for the WVIA instrument. Hence, they are investigated here only for the L1115-i system using the SDM calibration unit.

#### 4.3.1 Dependency of the isotope measurement precision on water vapour mixing ratio

The measurement precision of  $\delta^2\text{H}$  for the L1115-i instrument increases with increasing water vapour mixing ratio (Fig. 6a). This finding concurs with a higher signal-to-noise ratio for a larger number of molecules and is similar to the one found by Sturm and Knohl (2010) for WVIA. The  $\delta^{18}\text{O}$  precision however exhibits a different behaviour (Fig. 6b): the precision of  $\delta^{18}\text{O}$  increases with augmenting water vapour mixing ratios at very low water vapour mixing ratios, up to around 8000 ppmv, where it reaches a maximum. For water vapour mixing ratios above 8000 ppmv, the precision of  $\delta^{18}\text{O}$  decreases again. The decreasing precision for mixing ratios  $> 8000$  ppmv in the case of  $\delta^{18}\text{O}$  can be understood by considering the absorption spectrum. The absorption peak of  $\delta^{18}\text{O}$  is stronger than the one of  $\delta^2\text{H}$  (Helliker and Noone, 2010). Thus in the case of  $\delta^{18}\text{O}$  the sensitivity of the measurement can be affected by optical saturation at much lower water concentration values than in the case of  $\delta^2\text{H}$  (Gregor Hsiao, Picarro,

[Title Page](#)[Abstract](#)[Introduction](#)[Conclusions](#)[References](#)[Tables](#)[Figures](#)[◀](#)[▶](#)[Back](#)[Close](#)[Full Screen / Esc](#)[Printer-friendly Version](#)[Interactive Discussion](#)

personal communication, 2011). The water vapour mixing ratio dependency of  $\delta^{18}\text{O}$  for WVIA found in Sturm and Knohl (2010) and the results obtained for the new version L2130-i do not show such an optical saturation effect. For the WVIA the water vapour mixing ratio dependency is stronger in amplitude for  $\delta^{18}\text{O}$  compared to our results for L1115-i as shown by the dashed lines in Fig. 6. For  $\delta^2\text{H}$  the water vapour mixing ratio dependency of WVIA is practically identical to what is found here for L1115-i. With the new version L2130-i the precision is comparable, or even slightly better than in L1115-i (Table 5).

### 4.3.2 Dependency of the isotope measurement accuracy on water vapour mixing ratio

The average permil deviations ( $\Delta\delta^2\text{H}$  and  $\Delta\delta^{18}\text{O}$ ) expressed with respect to the calibrated isotope values of the four standards at 18 000 ppmv are shown in Fig. 7 as a function of water vapour mixing ratio for the L1115-i instrument. The dark blue dots (Fig. 7a, b) show the average isotope measurement bias dependency of water vapour mixing ratio using dried ambient air as a carrier gas. The standard deviation of the different runs performed in the corresponding water vapour mixing ratio range is represented by the shaded domain in Fig. 7. Biasing effects of up to 4‰ for  $\delta^2\text{H}$  and 2.5‰ for  $\delta^{18}\text{O}$  (Fig. 7a, b) due to varying amounts of water vapour in the gas samples can be observed with the L1115-i instrument. These dependencies on water vapour mixing ratio are considerable compared to the precision of the instrument (see Sect. 4.4) and they should be corrected especially when measurements are performed at a field site where water vapour mixing ratio can vary strongly (e.g. >10 000 ppmv in 12 h in Johnson et al., 2011). For L1115-i we use the following least square fits represented by the dark blue curves in Fig. 7:

$$\Delta\delta^2\text{H} = -6.4 \times 10^{-13}[\text{H}_2\text{O}]^3 + 1.6 \times 10^{-8}[\text{H}_2\text{O}]^2 + 1.9 \times 10^{-4}[\text{H}_2\text{O}] - 4.9 \quad (6)$$

$$\Delta\delta^{18}\text{O} = \frac{-1.2 \times 10^7}{[\text{H}_2\text{O}]^2} + \frac{1.6 \times 10^4}{[\text{H}_2\text{O}]} - 1.8 \quad (7)$$

<a href="#">Title Page</a>	
<a href="#">Abstract</a>	<a href="#">Introduction</a>
<a href="#">Conclusions</a>	<a href="#">References</a>
<a href="#">Tables</a>	<a href="#">Figures</a>
<a href="#">◀</a>	<a href="#">▶</a>
<a href="#">◀</a>	<a href="#">▶</a>
<a href="#">Back</a>	<a href="#">Close</a>
<a href="#">Full Screen / Esc</a>	

[Printer-friendly Version](#)

[Interactive Discussion](#)

## Characterisation of water vapour isotope measurements by laser spectroscopy

F. Aemisegger et al.

[Title Page](#)

[Abstract](#)

[Introduction](#)

[Conclusions](#)

[References](#)

[Tables](#)

[Figures](#)

◀

▶

◀

▶

[Back](#)

[Close](#)

[Full Screen / Esc](#)

[Printer-friendly Version](#)

[Interactive Discussion](#)

(~30 ppmv). The latter is only affected by memory effects from the walls of the tubing and the cavity. In the dried ambient air, however, the background water vapour mixing ratio influences the isotopic composition of the measured sample significantly at low water vapour mixing ratios. This results in a higher variability of the measurements especially at low water vapour mixing ratios. In principle, the effect of remaining ambient water vapour in the carrier gas can be corrected. However, for such a correction a good estimate of the true isotopic composition of the carrier gas is needed, which is difficult to obtain due to the high uncertainty of isotopic measurements at very low water vapour mixing ratios, especially for  $\delta^2\text{H}$  (Fig. 6). We estimated the isotopic composition of dried ambient air by performing calibration runs without pumping any liquid into the vaporiser. We found  $\delta^2\text{H}_{\text{dry}} = (-293 \pm 45) \text{ ‰}$  and  $\delta^{18}\text{O}_{\text{dry}} = (-47 \pm 2) \text{ ‰}$ . Due to these high uncertainties in the estimation of dried ambient air isotopic composition a correction for remaining ambient water vapour just introduces a higher uncertainty at low water vapour mixing ratios and is not useful to get a better water vapour dependency correction function. Even though using dried ambient air as a carrier gas implies the problem of residual ambient humidity, we use it for calibration in the field rather than air from a gas cylinder, because its composition in terms of other trace gases is the same as for the sample gas measured.

#### 4.4 Stability of water vapour isotope measurements

The stability of a laser spectroscopic system is an important characteristic, which allows to quantify the precision of the measurement system for given averaging times, the instrument internal drifts as well as the optimal inter-calibration time. Our analysis of stability is divided into two aspects: short-term drifts to quantify maximum precision and optimum averaging time, and long-term precision to determine an optimal calibration scheme for each instrument.

<a href="#">Title Page</a>	
<a href="#">Abstract</a>	<a href="#">Introduction</a>
<a href="#">Conclusions</a>	<a href="#">References</a>
<a href="#">Tables</a>	<a href="#">Figures</a>
<a href="#">◀</a>	<a href="#">▶</a>
<a href="#">◀</a>	<a href="#">▶</a>
<a href="#">Back</a>	<a href="#">Close</a>
<a href="#">Full Screen / Esc</a>	

[Printer-friendly Version](#)

[Interactive Discussion](#)

#### 4.4.1 Short-term stability

The short-term stability of the constant isotope signal in Fig. 8 is expressed in terms of the square root of the Allan variance (Sect. 3.4.1), the Allan deviation, as a function of averaging time. Consider for example the Allan plot for  $\delta^2\text{H}$  of L1115-i (dark blue crosses in Fig. 8a). The Allan deviation decreases towards higher averaging times up to a minimum, which is the optimum averaging time ( $\tau_0 = 10^3$  s) and then increases again for averaging times  $> \tau_0$ . These two stability domains, which are separated by the minimum of  $\sigma_A(\tau)$  in  $\tau_0$  can be observed in all the Allan curves of Fig. 8. The left side shows increasing precision with longer averaging times. This corresponds to a perfect white noise signal, as shown by the solid line. The latter is obtained from Allan deviations computed from a randomly generated white noise signal with the same variance as the measurements at the temporal resolution of the data acquisition. In theory, infinite averaging would thus lead to a perfectly stable system (Werle, 2011). In real systems, however, a minimum is reached at the optimum averaging time, after which the averaged signal is dominated by instrument drift. These drifts are due to low frequency variations in controlling elements of the spectrometer like temperature, pressure, laser current or varying environmental conditions, or due to slight changes in the properties of the calibration vapour.

The key characteristics of the Allan plot of the four investigated laser instruments such as the optimal integration time ( $\tau_0$ ), the Allan deviation at optimal integration time ( $\sigma_A^{\tau_0}$ ) as well as the Allan deviation at high temporal resolution ( $\sigma_A^{5\text{s}}$ ) are summarised in Table 6. For mesoscale meteorological applications an averaging time range of 15 min to 6 h is useful and thus precision values of the order of the numbers indicated in Table 6 for  $\sigma_A^{\tau_0}$  can be expected. For flux measurements high temporal resolution signals are needed with precisions of around  $\sigma_A^{5\text{s}}$  in Table 6. The precision of the WVIA is slightly higher than the one of the L1115-i instrument at small integration times. However, the minimum Allan deviation is reached later by the L1115-i signal and at higher integration times than 20 min stability is better, in particular for  $\delta^{18}\text{O}$ .

<a href="#">Title Page</a>	
<a href="#">Abstract</a>	<a href="#">Introduction</a>
<a href="#">Conclusions</a>	<a href="#">References</a>
<a href="#">Tables</a>	<a href="#">Figures</a>
<a href="#">◀</a>	<a href="#">▶</a>
<a href="#">◀</a>	<a href="#">▶</a>
<a href="#">Back</a>	<a href="#">Close</a>
<a href="#">Full Screen / Esc</a>	
<a href="#">Printer-friendly Version</a>	
<a href="#">Interactive Discussion</a>	

The stability performance of the WVIA found here is similar to the results by Sturm and Knohl (2010). The latest versions of the two instruments (L2130-i and WVIA-EP) show better performance in terms of precision. The L2130-i instrument has smaller Allan deviations than the L1115-i for all integration times and longer optimal integration times. The precision of the WVIA-EP is not improved with respect to WVIA for small integration times, however it is characterised by larger optimal averaging times and reaches higher precision than WVIA at longer integration times.

#### 4.4.2 Long-term stability

In addition to the short-term stability analysis, which provides reference numbers for precision and optimum averaging times of the instruments, long-term stability has to be investigated to determine the best possible calibration scheme. An analysis of long-term stability consists of a more detailed investigation of the effect of drifts on the measurements at the time scale of a few hours to a few days. For this purpose WS 6 was measured every 30 min over a time period of two weeks (Sect. 3.4.2). The long-term stability of the  $\delta^{18}\text{O}$  and  $\delta^2\text{H}$  calibration time series of both instruments is then assessed by applying a bias correction, which is recalculated at varying inter-calibration intervals. Because only one standard is measured here the calibration consists of a simple bias correction. The bias correction is computed by linearly interpolating between two consecutive calibration runs, which are considered for the bias correction. This procedure is illustrated for the  $\delta^2\text{H}$  signal in Fig. 9a, b for L1115-i and WVIA, respectively. Here, the color coding refers to the calibration interval and not to the instrument type. Sub-daily calibration (light blue curve in Fig. 9) allows to correct drifts more accurately than if calibration is only done every few days (dark red curve in Fig. 9). The maximum amplitude of the corrections is rather small with  $\sim 1\text{‰}$  for  $\delta^2\text{H}$  and  $\sim 0.5\text{‰}$  for  $\delta^{18}\text{O}$ .

The observed drifts in both L1115-i and WVIA are due to low frequency changes in instrument characteristics. They can be limited by applying regular calibration. In this experiment artificial drifting effects introduced by the calibration system itself cannot

[Title Page](#)  
[Abstract](#) [Introduction](#)  
[Conclusions](#) [References](#)  
[Tables](#) [Figures](#)  
[◀](#) [▶](#)  
[◀](#) [▶](#)  
[Back](#) [Close](#)  
[Full Screen / Esc](#)

[Printer-friendly Version](#)  
[Interactive Discussion](#)



be excluded. However, the bias correction time series of the two instruments are uncorrelated (Fig. 9a, b), which is a good indication that instrument drifts prevail over the calibration system drifts.

A certain memory in the amplitude and sign of the bias correction time series for both instruments (Fig. 9a, b) can be observed. To find out for how long on average a given bias correction is still useful, the autocorrelation functions of the time series of the calibration runs were computed and are shown in Fig. 10. The minimum number of lags at which the autocorrelation function of the isotope signal of a given instrument reaches 0 gives an indication about the maximum time range of validity of a bias correction.

5 For the L1115-i  $\delta^{18}\text{O}$  signal and  $\delta^2\text{H}$  signal it is 15 h and 2.5 days, respectively. For the WVIA it is 2 days, and 1.5 days for the  $\delta^2\text{H}$  and  $\delta^{18}\text{O}$  signals, respectively. Inter-calibration periods longer than these durations do not improve the measurements.

10

A second characteristic of the calibration scheme apart from the maximum inter-calibration time is the root mean square error (RMSE) of the calibrated time series.

15 The dependency of the RMSE on the inter-calibration time is shown in Fig. 11. The uncertainty of the isotope signals increases exponentially with increasing inter-calibration time for both instruments and both isotopes. For  $\delta^2\text{H}$  the uncertainty increase is of similar extent for both instruments. The L1115-i accuracy of  $\delta^{18}\text{O}$  is however much better than the one of WVIA. Accurate and precise  $\delta^{18}\text{O}$  measurements are essential for good quality derived deuterium excess ( $d = \delta^2\text{H} - 8\delta^{18}\text{O}$ ) signals. Thus, when choosing the optimum inter-calibration time the  $\delta^{18}\text{O}$  accuracy should be kept in mind.

20

#### 4.4.3 Calibration strategy

Ideally, in order to avoid any effect of drift and to obtain the best possible accuracy of the measurements, the instruments should be calibrated at a frequency corresponding to the optimum inter-calibration time, for a duration corresponding to the optimum averaging time. However, a trade-off has to be made between minimum drift, maximum precision of the calibration runs and minimum measurement time consumption for calibration. Calibration with the standard delivery module built for the L1115-i system

[Title Page](#)

[Abstract](#)

[Introduction](#)

[Conclusions](#)

[References](#)

[Tables](#)

[Figures](#)

◀

▶

◀

▶

[Back](#)

[Close](#)

[Full Screen / Esc](#)

[Printer-friendly Version](#)

[Interactive Discussion](#)

is relatively measurement time consuming due to the long equilibration phase in the vaporiser. With a two-point calibration run every 12 h using two different standards at three different water vapour mixing ratios, one hour calibration time per day is needed in total. With such a calibration frequency the precision of the L1115-i signal averaged to

5 15 min is  $\sigma_A(\delta^2\text{H}) = 0.05\text{‰}$  and  $\sigma_A(\delta^{18}\text{O}) = 0.01\text{‰}$  and the accuracy is 0.25 ‰ for  $\delta^2\text{H}$  and 0.09 ‰ for  $\delta^{18}\text{O}$ . With calibration runs performed every hour using the WVISS, the precision of the WVISS can be expected to be  $\sigma_A(\delta^2\text{H}) = 0.05\text{‰}$  and  $\sigma_A(\delta^{18}\text{O}) = 0.03\text{‰}$  and the accuracy becomes 0.08 ‰ for  $\delta^2\text{H}$  and 0.07 ‰ for  $\delta^{18}\text{O}$ .

## 4.5 Response time

10 The sampling system, the external tubing and the optical cavity in the instrument smoothen the measurement signal by retarding some molecules due to adsorption and desorption of the sample gas at the walls (see Sect. 3.5). The response times  $\tau_{\text{ads}}$  for  $\delta^2\text{H}$ ,  $\delta^{18}\text{O}$  and  $\text{H}_2\text{O}$  averaged over all performed step changes in water vapour signal differ and amount to 36 s, 25 s, and 15 s for L1115-i and 4.5 s, 3 s and 2.9 s for WVISS,  
15 respectively. Schmidt et al. (2010) found that the response time of  $\delta^2\text{H}$  lags behind the one of  $\delta^{18}\text{O}$  by a factor of 1.7–3.3 using a PFA tubing, which is more than the factor of  $1.5 \pm 0.1$  found here for both L1115-i and WVISS also using PFA tubing. The difference in the response times of the isotopes has implications for the computation of deuterium excess. During a step change in water vapour mixing ratio and isotope concentration  
20 the signals of water vapour mixing ratio and the two heavy isotopes reach the new target values, when the equilibrium between the pipe gas and the adsorbed phase on the tubing wall has been re-established. The longer response times for the heavy isotopes compared to the bulk water concentration is an evidence for longer interaction time scales of the heavy isotopes with the tubing and cavity walls and thus a higher affinity  
25 with the material.

The 5–10 times smaller response times of WVISS compared to L1115-i indicate that the influence of the external tubing on the memory effect of the measurement systems

[Title Page](#)

[Abstract](#)

[Introduction](#)

[Conclusions](#)

[References](#)

[Tables](#)

[Figures](#)

◀

▶

[Back](#)

[Close](#)

[Full Screen / Esc](#)

[Printer-friendly Version](#)

[Interactive Discussion](#)

**Characterisation of water vapour isotope measurements by laser spectroscopy**

F. Aemisegger et al.

[Title Page](#)[Abstract](#)[Introduction](#)[Conclusions](#)[References](#)[Tables](#)[Figures](#)[◀](#)[▶](#)[◀](#)[▶](#)[Back](#)[Close](#)[Full Screen / Esc](#)[Printer-friendly Version](#)[Interactive Discussion](#)

up cases. In general, temperature effects observed in Fig. 12 are small in the range of 30 °C to 120 °C. Thus, the sampling line heating is needed primarily to avoid condensation and does not reduce response times significantly.

For both laser systems used here we found that it is not the acquisition time which determines the highest possible temporal resolution of the measurements but the exchange rate of the cavity and the interaction timescale of the water molecules with the tubing and cavity walls. Thus, the choice of the tubing material and the flow rate through the sampling system are central aspects of an isotope measurement setup. A good knowledge of the response time distribution of each isotope signal allows to correct for biases introduced by the sampling system and provides a framework for the uncertainty assessment of high frequency variations in  $\delta^{18}\text{O}$ ,  $\delta^2\text{H}$  and deuterium excess.

## 4.6 Comparative ambient air measurements

As a verification of the laboratory characterisation experiments comparative ambient air measurements were done during seven days in July 2011 in the city of Zurich on the roof of a tower building (Sect. 3.6). The L1115-i was calibrated using the SDM by performing two calibrations per day at 03:00 p.m. and 03:00 a.m. for  $\sim 1$  h in total using WS 6 and WS 7 (Table 2). Calibrations were performed at the ambient water vapour mixing ratio conditions as well as 3000 ppmv above and 3000 ppmv below ambient water vapour mixing ratios. If variations in water vapour mixing ratio during the day were  $> 1000$  ppmv the corrections found in Sect. 4.3 Eqs. (6) and (7) were applied. The average standard deviation of the calibration runs was 0.8‰ for  $\delta^2\text{H}$  and 0.2‰ for  $\delta^{18}\text{O}$ .

For the WVIA, calibration runs were performed every 15 min for 2 min using WS 6 (Table 2). The water vapour mixing ratio correction function was determined once on 19 July and once on 26 July using the WVISS by measuring WS 6 at different water vapour mixing ratios in the range 5000–25 000 ppmv. The average standard deviation of the calibration runs was 1.3‰ for  $\delta^2\text{H}$  and 0.6‰ for  $\delta^{18}\text{O}$ .

[Title Page](#)[Abstract](#)[Introduction](#)[Conclusions](#)[References](#)[Tables](#)[Figures](#)[◀](#)[▶](#)[◀](#)[▶](#)[Back](#)[Close](#)[Full Screen / Esc](#)[Printer-friendly Version](#)[Interactive Discussion](#)

**Characterisation of water vapour isotope measurements by laser spectroscopy**

F. Aemisegger et al.

[Title Page](#)[Abstract](#)[Introduction](#)[Conclusions](#)[References](#)[Tables](#)[Figures](#)[◀](#)[▶](#)[◀](#)[▶](#)[Back](#)[Close](#)[Full Screen / Esc](#)[Printer-friendly Version](#)[Interactive Discussion](#)

the new Picarro version L2130-i. No methane measurements were done during this campaign. The cross-talk effect between water isotope measurements in water vapour and methane, if relevant, could not be corrected for.

## 5 Conclusions

- 5 This paper presents a characterisation study of laser spectroscopic measurements of stable isotopes in ambient water vapour. We used two commercial versions of two laser spectroscopic systems as well as comparative IRMS measurements. The laser spectroscopic instruments used were two systems by Picarro (versions L1115-i and L2130-i) and two systems by Los Gatos Research (WVIA, WVIA-EP). The main properties of the laser measurement systems investigated here were biases due to water concentration effects, precision and accuracy in terms of short and long-term stability, and response times.
- 10

The assessments presented in this paper were all pursued with the final aim of obtaining a comprehensive picture of the uncertainty of high frequency water vapour isotope measurements using field-deployable laser spectroscopic instruments. We found that a large part of the measurement uncertainty depends on how the instruments are calibrated, more specifically on the calibration technique and strategy.

The inherent precision of the Picarro L1115-i instrument is dependent on water vapour mixing ratio. In general, we found higher measurement uncertainties for lower water vapour mixing ratios. This represents the basic uncertainty of the measurement. Other uncertainty sources are then superimposed and depend on the sampling procedure and calibration. The uncertainty of the calibration vapour production system adds to the basic measurement uncertainty. An overall estimate of the bottom up uncertainty is difficult to obtain as the different error components cannot be estimated independently. The assessments of the different uncertainty components however allow us to determine an optimal calibration procedure for the two instruments, which is a trade-off between maximum ambient air measurement time, maximum precision

[Title Page](#)

[Abstract](#)

[Introduction](#)

[Conclusions](#)

[References](#)

[Tables](#)

[Figures](#)

[◀](#)

[▶](#)

[Back](#)

[Close](#)

[Full Screen / Esc](#)

[Printer-friendly Version](#)

[Interactive Discussion](#)

of the calibration run, which typically requires long calibration runs (10–30 min) and minimum inter-calibration time to regularly update calibration factors.

The precision at optimum averaging time is  $\sigma_A^{\tau_0=15\text{ min}}(\delta^2\text{H}) = 0.05\text{ ‰}$  and  $\sigma_A^{\tau_0=30\text{ min}}(\delta^{18}\text{O}) = 0.01\text{ ‰}$  for L1115-i and  $\sigma_A^{\tau_0=10\text{ min}}(\delta^2\text{H}) = 0.05\text{ ‰}$  and  $\sigma_A^{\tau_0=7\text{ min}}(\delta^{18}\text{O}) = 0.03\text{ ‰}$  for WVIA at 15 700 ppmv water vapour mixing ratio. The precision of the instruments decreases linearly with increasing depletion of the samples. The measurement precision of both instruments is smaller in the new versions of the two instruments L2130-i and WVIA-EP. In both new instrument versions Allan deviations at optimum averaging time are smaller compared to the ones found for the previous versions.

We performed two top-down assessments of uncertainty by comparing the calibration measurements of 12 standards as well as ambient air measurement by the WVIA and L1115-i instruments. From the roof top measurements we obtained root mean square deviations between the two instruments of  $\text{RMSE}(\delta^2\text{H}) = 2.3\text{ ‰}$  and  $\text{RMSE}(\delta^{18}\text{O}) = 0.5\text{ ‰}$ . The delta-scale linearity experiment showed that repeated measurements of 12 standards lead to uncertainties of on average 1.7 ‰ (1.0 ‰) for  $\delta^2\text{H}$  and 0.4 ‰ (0.5 ‰) for  $\delta^{18}\text{O}$  for L1115-i (WVIA). IRMS is typically characterised by similar or slightly smaller uncertainties than found here for the L1115-i and WVIA systems.

The uncertainty of deuterium excess resulting from ambient measurements done with the well characterised laser spectrometers used here was 3.1 ‰. This uncertainty will probably be reduced in upcoming versions of commercial instruments, owing to improved spectral fitting algorithms with respect to water vapour mixing ratio dependencies and interfering trace gases.

In summary, from the experiments presented in this paper we can formulate the following recommendations for the use of laser spectrometric systems to measure ambient water vapour isotopes during field campaigns:

[Title Page](#)[Abstract](#)[Introduction](#)[Conclusions](#)[References](#)[Tables](#)[Figures](#)[◀](#)[▶](#)[◀](#)[▶](#)[Back](#)[Close](#)[Full Screen / Esc](#)[Printer-friendly Version](#)[Interactive Discussion](#)

---

**Characterisation of  
water vapour isotope  
measurements by  
laser spectroscopy**

F. Aemisegger et al.

<a href="#">Title Page</a>	
<a href="#">Abstract</a>	<a href="#">Introduction</a>
<a href="#">Conclusions</a>	<a href="#">References</a>
<a href="#">Tables</a>	<a href="#">Figures</a>
<a href="#">◀</a>	<a href="#">▶</a>
<a href="#">◀</a>	<a href="#">▶</a>
<a href="#">Back</a>	<a href="#">Close</a>
<a href="#">Full Screen / Esc</a>	
<a href="#">Printer-friendly Version</a>	
<a href="#">Interactive Discussion</a>	

5      1. Calibration runs should be done regularly and ideally at the same water vapour mixing ratio as the measurements. For the L1115-i we perform a two point calibration run every 12 h using 2 different standards at 3 different water vapour mixing ratios, which takes 1 h calibration time per day in total. For the WVIA calibration runs should be performed hourly for 5–10 min to obtain the highest possible accuracy.

10     2. Water vapour mixing ratio effects should be quantified for old versions of the laser spectrometers. These effects are different for each instrument and the correction functions found in this study have no general validity. In the new version of the Picarro instrument (L2130-i) however, the water vapour mixing ratio dependency of isotope measurements is very small and corrections are not necessary except if measurements are performed in very dry conditions.

15     3. Dried ambient air is recommended as a carrier gas for calibration because its trace gas composition is equivalent to the measured gas sample. Residual ambient water can be a problem when calibrating at very low water vapour mixing ratios. In this case laboratory tests with other carrier gases can be helpful.

20     4. If high frequency measurements are used, response time differences in  $\delta^{18}\text{O}$  and  $\delta^2\text{H}$  should be accounted for. These depend on the setup and the tubing material used and have to be quantified experimentally. We found that response times were 1.5 times larger for  $\delta^2\text{H}$  than for  $\delta^{18}\text{O}$  and 10 times larger for L1115-i than for WVIA. The response times of the measured signals depend on the exchange rate of the measurement cell and tubing systems as well as the material affinity of the isotopes. However, no clear dependency of the response times on tubing temperature was found.

25     5. To obtain high accuracy water vapour mixing ratio measurements with uncertainties smaller than 500 ppmv regular calibration of the water vapour mixing ratio measurements are suggested.

**Acknowledgements.** We thank Roland Werner from the Institute of Agricultural Sciences, ETH for the IRMS measurements of our standards, Aaron van Pelt and Gregor Hsiao from Picarro and Doug Baer from LGR for technical support as well as Edwin Hausmann and Uwe Weers for technical help in the lab. Patrick Sturm and Alexander Knohl were funded by a Marie Curie 5 Excellence Grant of the European Commission (Project No: MEXT-CT-2006-042268).

## References

Allan, D. W.: Statistics of atomic frequency standards, *P. IEEE*, 54, 221–230, doi:10.1109/PROC.1966.4634, 1966. 1609

Araguas, L. A., Danesi, P., Froehlich, K., and Rozanski, K.: Global monitoring of the isotopic 10 composition of precipitation, *J. Radioanal. Nucl. Ch.*, 205, 189–200, 1996. 1599

Baer, D. S., Paul, J. B., Gupta, M., and O'Keefe, A.: Sensitive absorption measurements in the near-infrared region using off-axis integrated-cavity output spectroscopy, *Appl. Phys. B-Lasers O.*, 75, 261–265, 2002. 1600, 1602, 1603

Brand, W. A., Geilmann, H., Crosson, E. R., and Rella, C. W.: Cavity ring-down spectroscopy 15 versus high-temperature conversion isotope ratio mass spectrometry; a case study on  $\delta^2\text{H}$  and  $\delta^{18}\text{O}$  of pure water samples and alcohol/water mixtures, *Rapid Commun. Mass. Sp.*, 23, 1879–1884, doi:10.1002/rcm.4083, 2009. 1600

Ciais, P. and Jouzel, J.: Deuterium and oxygen 18 in precipitation: isotopic model, including mixed cloud processes, *J. Geophys. Res.-Atmos.*, 99, 16793–16803, 1994. 1599

Craig, H.: Isotopic variations in meteoric waters, *Sci. J.*, 133, 1702–1703, 1961. 1599

Crosson, E. R.: A cavity ring-down analyzer for measuring atmospheric levels of methane, carbon dioxide and water vapor, *Appl. Phys. B-Lasers O.*, 92, 403–408, 2008. 1600, 1602, 1603

Dansgaard, W.: Stable isotopes in precipitation, *Tellus*, 16, 436–468, 1964. 1599

Dansgaard, W., Johnsen, S. J., Clausen, H. B., Dahl-Jensen, D., Gundestrup, N. S., Hammer, C. U., Hvidberg, C. S., Steffensen, J. P., Sveinbjörnsdóttir, A. E., Jouzel, J., and Bond, G.: Evidence for general instability in past climate from a 250-kyr ice-core record, *Nature*, 364, 218–220, 1993. 1599

Dongmann, G., Nürnberg, H. W., Förstel, H., and Wagener, K.: On the enrichment of  $\text{H}_2^{18}\text{O}$  in 30 the leaves of transpiring plants, *Radiat. Environ. Bioph.*, 11, 41–52, 1974. 1599

Title Page

Abstract

Introduction

Conclusions

References

Tables

Figures

◀

▶

◀

▶

Back

Close

Full Screen / Esc

Printer-friendly Version

Interactive Discussion

## Characterisation of water vapour isotope measurements by laser spectroscopy

F. Aemisegger et al.

[Title Page](#)

[Abstract](#)

[Introduction](#)

[Conclusions](#)

[References](#)

[Tables](#)

[Figures](#)

◀

▶

◀

▶

[Back](#)

[Close](#)

[Full Screen / Esc](#)

[Printer-friendly Version](#)

[Interactive Discussion](#)

## Characterisation of water vapour isotope measurements by laser spectroscopy

F. Aemisegger et al.

[Title Page](#)

[Abstract](#)

[Introduction](#)

[Conclusions](#)

[References](#)

[Tables](#)

[Figures](#)

◀

▶

[Back](#)

[Close](#)

[Full Screen / Esc](#)

[Printer-friendly Version](#)

[Interactive Discussion](#)

on Earth Through Isotope Mapping, edited by: West, J. B., Chap. 4, 71–87, Springer Science, 2010. 1599, 1616

Horita, J. and Kendall, C.: Stable isotope analysis of water and aqueous solutions by conventional dual-inlet mass spectrometry, in: Handbook of Stable Isotope Analytical Techniques, edited by: de Groot, P. A., Vol. 1, Chap. 1, 1–37, Elsevier, 2004. 1600

5 IAEA: Reference Sheet for VSMOW2 and SLAP2 international measurement standards, International Atomic Energy Agency (IAEA), 2009. 1602, 1607, 1614, 1636, 1638

Iannone, R. Q.: Development of a near-infrared Optical Feedback Cavity Enhanced Absorption Spectrometer (OF-CEAS) for atmospheric water vapor isotope ratio ( $^{18}\text{O}/^{16}\text{O}$ ,  $^{17}\text{O}/^{16}\text{O}$  and  $^{2}\text{H}/^{1}\text{H}$ ) measurements, Ph.D. thesis, University of Groningen, 2009. 1603

10 Iannone, R. Q., Romanini, D., Kassi, S., Meijer, H. A. J., and Kerstel, E. R. T.: A microdrop generator for the calibration of a water vapor isotope ratio spectrometer, *J. Atmos. Ocean Tech.*, 26, 1275–1288, doi:10.1175/2008JTECHA1218.1, 2009.

Johnson, L. R., Sharp, Z. D., Galewsky, J., Strong, M., Van Pelt, A. D., Dong, F., and Noone, D.: 15 Hydrogen isotope correction for laser instrument measurement bias at low water vapor concentration using conventional isotope analyses: application to measurements from Mauna Loa Observatory, Hawaii, *Rapid Commun. Mass. Sp.*, 25, 608–616, doi:10.1002/rcm.4894, 2011. 1600, 1604, 1617

Johnsen, S. J., Dahl-Jensen, D., Gundestrup, N., Steffensen, J. P., Clausen, H. B., Miller, H., 20 Masson-Delmotte, V., Sveinbjörnsdóttir, A. E., and White, J.: Oxygen isotope and palaeotemperature records from six Greenland ice-core stations: Camp Century, Dye-3, GRIP, GISP2, Renland and NorthGRIP, *J. Quaternary Sci.*, 16, 299–307, 2001. 1599

Jouzel, J., Alley, R. B., Cuffey, K. M., Dansgaard, W., Grootes, P., Hoffmann, G., Johnsen, S. J., Koster, R. D., Peel, D., Shuman, C. A., Stievenard, M., Stuiver, M., and White, J.: Validity of 25 the temperature reconstruction from water isotopes in ice cores, *J. Geophys. Res.-Oceans*, 102, 26471–26487, 1997. 1599

Kerstel, E. R. T. and Gianfrani, L.: Advances in laser-based isotope ratio measurements: selected applications, *Appl. Phys. B-Lasers O.*, 92, 439–449, 2008. 1600

Kerstel, E. R. T., Iannone, R. Q., Chenevier, M., Kassi, S., Jost, H. J., and Romanini, D.: 30 A water isotope ( $^{2}\text{H}$ ,  $^{17}\text{O}$ , and  $^{18}\text{O}$ ) spectrometer based on optical feedback cavity-enhanced absorption for in situ airborne applications, *Appl. Phys. B-Lasers O.*, 85, 397–406, doi:10.1007/s00340-006-2356-1, 2006. 1600

Lee, J.-E. and Fung, I.: “Amount effect” of water isotopes and quantitative analysis of post-

**Characterisation of water vapour isotope measurements by laser spectroscopy**

F. Aemisegger et al.

condensation processes, *Hydrol. Process.*, 22, 1–8, doi:10.1002/hyp.6637, 2008. 1599

Lee, X., Sargent, S., Smith, R., and Tanner, B.: In situ measurement of the water vapor  $^{18}\text{O}/^{16}\text{O}$  isotope ratio for atmospheric and ecological applications, *J. Atmos. Ocean Tech.*, 22, 555–565, 2005. 1600

5 Lis, G., Wassenaar, L. I., and Hendry, M. J.: High-precision laser spectroscopy D/H and  $^{18}\text{O}/^{16}\text{O}$  measurements of microliter natural water samples, *Anal. Chem.*, 80, 287–293, 2008.

Oura, K., Lifshits, V. G., Saranin, A. A., Zotov, A. V., and Katayama, M.: *Surface Science: An Introduction*, Springer, Berlin, 2003. 1624

10 Paldus, B. A. and Kachanov, A. A.: An historical overview of cavity-enhanced methods, *Can. J. Phys.*, 83, 975–999, 2005. 1600, 1603

Pfahl, S. and Wernli, H.: Air parcel trajectory analysis of stable isotopes in water vapor in the eastern Mediterranean, *J. Geophys. Res.-Atmos.*, 113, D20104, doi:10.1029/2008JD009839, 2008. 1599

15 Rambo, J., Lai, C.-T., Farlin, J., Schroeder, M., and Bible, K.: On-site calibration for high precision measurements of water vapor isotope ratios using off-axis cavity-enhanced absorption spectroscopy, *J. Atmos. Ocean Tech.*, 28, 1448–1457, doi:10.1175/JTECH-D-11-00053.1, 2011. 1600

20 Rothman, L. S., Gordon I. E., Barbe, A., Chris Benner, D., Bernath, P. F., Birk, M., Boudon, V., Brown, L. R., Campargue, A., Champion, J.-P., Chance, K., Coudert, L. H., Dana, V., Devi, V. M., Fally, S., Flaud, J.-M., Gamache, R. R., Goldmann, A., Jacquemart, D., Kleiner, I., Lacome, N., Lafferty, W. J., Mandin, J.-Y., Massie, S. T., Mikhailenko, S. N., Miller, C. E., Moazzen-Ahmadi, N., Naumenko, O. V., Nikitin, A. V., Orphal, J., Perevalov, V. I., Perrin, A., Predoi-Cross, A., Rinsland, C. P., Rotger, M., Simečková, M., Smith, M. A. H., Sung, K., Tashkun, S. A., Tennyson, J., Toth, R. A., Vandaele, A. C., and Vander Auwera, J.: The HITRAN 2008 molecular spectroscopic database, *J. Quant. Spectrosc. Ra.*, 110, 533–572, 2009. 1626

25 Sayres, D. S., Moyer, E. J., Hanisco, T. F., St Clair, J. M., Keutsch, F. N., O'Brien, A., Allen, N. T., Lapson, L., Demusz, J. N., Rivero, M., Martin, T., Greenberg, M., Tuozzolo, C., Engel, G. S., Kroll, J. H., Paul, J. B., and Anderson, J. G.: A new cavity based absorption instrument for detection of water isotopologues in the upper troposphere and lower stratosphere, *Rev. Sci. Instrum.*, 80, 044102, doi:10.1063/1.3117349, 2009. 1600

30 Schmidt, M., Maseyk, K., Lett, C., Biron, P., Richard, P., Bariac, T., and Seibt, U.: Concentration effects on laser-based  $\delta^{18}\text{O}$  and  $\delta^2\text{H}$  measurements and implications for the calibration of

[Title Page](#)[Abstract](#)[Introduction](#)[Conclusions](#)[References](#)[Tables](#)[Figures](#)[◀](#)[▶](#)[◀](#)[▶](#)[Back](#)[Close](#)[Full Screen / Esc](#)[Printer-friendly Version](#)[Interactive Discussion](#)

**Characterisation of  
water vapour isotope  
measurements by  
laser spectroscopy**

F. Aemisegger et al.

vapour measurements with liquid standards, *Rapid Commun. Mass. Sp.*, 24, 3553–3561, doi:10.1002/rcm.4813, 2010. 1600, 1610, 1618, 1623

Sodemann, H., Masson-Delmotte, V., Schwierz, C., Vinther, B. M., and Wernli, H.: Interannual variability of Greenland winter precipitation sources: 2. Effects of North Atlantic Oscillation variability on stable isotopes in precipitation, *J. Geophys. Res.-Atmos.*, 113, D12111, doi:10.1029/2007JD009416, 2008. 1599

Strong, M. Z. D., Sharp, D., and Gutzler, D. S.: Diagnosing moisture transport using D/H ratios of water vapor, *Geophys. Res. Lett.*, 34, L03404, doi:10.1029/2006GL028307, 2007. 1600

Sturm, P. and Knohl, A.: Water vapor  $\delta^2\text{H}$  and  $\delta^{18}\text{O}$  measurements using off-axis integrated cavity output spectroscopy, *Atmos. Meas. Tech.*, 3, 67–77, doi:10.5194/amt-3-67-2010, 2010. 1600, 1601, 1610, 1616, 1617, 1621, 1647

Uemura, R., Matsui, Y., Yoshimura, K., Motoyama, H., and Yoshida, N.: Evidence of deuterium excess in water vapor as an indicator of ocean surface conditions, *J. Geophys. Res.-Atmos.*, 113, D19114, doi:10.1029/2008JD010209, 2008. 1599

Wang, L., Caylor, K. K., and Dragoni, D.: On the calibration of continuous, high-precision  $\delta^{18}\text{O}$  and  $\delta^2\text{H}$  measurements using an off-axis integrated cavity output spectrometer, *Rapid Commun. Mass Sp.*, 23, 530–536, doi:10.1002/rcm.3905, 2009.

Wen, X. F., Sun, X. M., Zhang, S. C., Yu, G. R., Sargent, S. D., and Lee, X.: Continuous measurement of water vapor D/H and  $^{18}\text{O}/^{16}\text{O}$  isotope ratios in the atmosphere, *J. Hydrol.*, 349, 489–500, 2008.

Werle, P.: Accuracy and precision of laser spectrometers for trace gas sensing in the presence of optical fringes and atmospheric turbulence., *Appl. Phys. B-Lasers O.*, 102, 313–329, 2011. 1609, 1620

Yakir, D. and Wang, X.-F.: Fluxes of  $\text{CO}_2$  and water between terrestrial vegetation and the atmosphere estimated from isotope measurements, *Nature*, 380, 515–517, 1996. 1600

Yepez, E. A., Williams, D. G., Scott, R. L., and Lin, G.: Partitioning overstory and understory evapotranspiration in a semiarid savanna woodland from the isotopic composition of water vapor, *Agr. Forest Meteorol.*, 119, 53–68, 2003. 1600

[Title Page](#)[Abstract](#)[Introduction](#)[Conclusions](#)[References](#)[Tables](#)[Figures](#)[◀](#)[▶](#)[Back](#)[Close](#)[Full Screen / Esc](#)[Printer-friendly Version](#)[Interactive Discussion](#)

## Characterisation of water vapour isotope measurements by laser spectroscopy

F. Aemisegger et al.

**Table 1.** Properties and technical details of the L1115-i, L2130-i (Picarro) and the WVIA (Los Gatos) laser systems. The WVIA-EP instrument has a smaller cavity than the WVIA, different ring-down times, laser path lengths but similar power consumption (200 W).

Properties	Picarro	Los Gatos
Technology	CRDS <sup>1</sup>	OA-ICOS <sup>2</sup>
Spectral domain	7183.5–7184 in steps of 0.01 $\text{cm}^{-1}$	7199.9–7200.4 $\text{cm}^{-1}$
Absorption path length	~20 km	~7 km
Ring down time	40 $\mu\text{s}$	24 $\mu\text{s}$
Cavity size	35 ccm	~830 ccm
Cavity pressure	$46.66 \pm 0.03 \text{ hPa}$	$50 \pm 0.007 \text{ hPa}$
Cavity temperature	$80 \pm 0.002^\circ\text{C}$	$\sim 47^\circ\text{C}$
Pumping rate	$25 \text{ ml min}^{-1}$	$500\text{--}800 \text{ ml min}^{-1}$
Cavity exchange rate	8 s	2–3 s
Measurement frequency	0.5 Hz (1 Hz <sup>*</sup> )	2 Hz
$\text{H}_2\text{O}$ range	6000 to 26 000 ppmv	4000 to 60 000 ppmv <sup>**</sup>
Volume	~130 l	~200 l
Power consumption	~300 W with calibration 500 W	~180 W (WVIA), 300 W (WVISS)

<sup>1</sup> cavity ring-down spectroscopy

<sup>2</sup> off-axis integrated cavity output spectroscopy

\* L2130-i

\*\* non-condensing

**Table 2.** Isotopic composition (in ‰) of the International IAEA standards and working standards (WS) used for the characterisation of the laser systems. The indicated isotopic  $\delta$  values of working standards 1–12 were measured with IRMS.

Standard	IRMS		
	name	$\delta^2\text{H}$ [‰]	$\delta^{18}\text{O}$ [‰]
IAEA VSMOW2		0 $\pm$ 0.30	0 $\pm$ 0.02*
IAEA SLAP2		-427.50 $\pm$ 0.30	-55.50 $\pm$ 0.02*
IAEA GISP2		-189.50 $\pm$ 1.2	-24.76 $\pm$ 0.09*
WS 1		-107.32 $\pm$ 1.1	-14.35 $\pm$ 0.04
WS 2		-140.03 $\pm$ 1.93	-18.42 $\pm$ 0.10
WS 3		-172.52 $\pm$ 1.11	21.46 $\pm$ 0.14
WS 4		-79.29 $\pm$ 0.62	-5.24 $\pm$ 0.25
WS 5		-188.13 $\pm$ 1.57	-24.72 $\pm$ 0.14
WS 6		-78.68 $\pm$ 0.19	-10.99 $\pm$ 0.12
WS 7		-153.90 $\pm$ 1.06	-24.89 $\pm$ 0.73
WS 8		-256.11 $\pm$ 0.85	-46.02 $\pm$ 0.82
WS 9		-166.74 $\pm$ 0.35	-70.19 $\pm$ 2.74
WS 10		14.89 $\pm$ 0.61	3.63 $\pm$ 0.35
WS 11		-80.27 $\pm$ 0.82	-11.21 $\pm$ 0.24
WS 12		-28.96 $\pm$ 0.70	2.27 $\pm$ 0.52

\* IAEA standards' composition as stated in IAEA (2009).

## Characterisation of water vapour isotope measurements by laser spectroscopy

F. Aemisegger et al.

[Title Page](#)

[Abstract](#)

[Introduction](#)

[Conclusions](#)

[References](#)

[Tables](#)

[Figures](#)

[◀](#)

[▶](#)

[◀](#)

[▶](#)

[Back](#)

[Close](#)

[Full Screen / Esc](#)

[Printer-friendly Version](#)

[Interactive Discussion](#)



## Characterisation of water vapour isotope measurements by laser spectroscopy

F. Aemisegger et al.

**Table 3.** Results from the delta scale linearity experiment. The two laser systems L1115-i and WVIA were compared to IRMS using ten standards which were measured on all the instruments twice (run 1 and run 2). The average difference over the ten standards for the different instrument combinations are listed.  $\overline{\sigma_s}$  indicates the average standard deviation of the measurements over all working standard runs.

Instrument combination	$\delta^2\text{H}$ [%]	$\delta^{18}\text{O}$ [%]
(a) L1115-i vs. WVIA	0.8±0.9	0.4±0.5
(b) L1115-i vs. IRMS	1.2±1.4	0.6±0.9
(c) WVIA vs. IRMS	0.7±1.0	0.7±1.4
(d) L1115-i 1 vs. L1115-i 2	1.9±1.6	0.2±0.2
(e) WVIA 1 vs. WVIA 2	0.8±0.6	0.2±0.2
(f) L1115-i $\overline{\sigma_s}$	1.7±0.4	0.5±0.1
(g) WVIA $\overline{\sigma_s}$	1.0±0.2	0.4±0.1
(h) IRMS $\overline{\sigma_s}$	0.9±0.5	0.4±0.7

[Title Page](#)  
[Abstract](#) [Introduction](#)  
[Conclusions](#) [References](#)  
[Tables](#) [Figures](#)  
[◀](#) [▶](#)  
[◀](#) [▶](#)  
[Back](#) [Close](#)  
[Full Screen / Esc](#)

[Printer-friendly Version](#)  
[Interactive Discussion](#)

## Characterisation of water vapour isotope measurements by laser spectroscopy

F. Aemisegger et al.

**Table 4.** Uncertainty in calibration factors following IAEA (2009). The normalisation slopes for both isotopes were determined for two calibration runs 1 ( $f_1$ ) and 2 ( $f_2$ ) using VSMOW2 and SLAP2 as reference standards. The intercepts of the calibrations from the two runs ( $b_1$ ) and ( $b_2$ ) are the measured VSMOW2 raw values of the laser instruments.

Calibration factors	L1115-i		WVIA	
	$\delta^2\text{H}$	$\delta^{18}\text{O}$	$\delta^2\text{H}$	$\delta^{18}\text{O}$
$f_1$ [–]	$1.064 \pm 0.009$	$1.113 \pm 0.008$	$0.995 \pm 0.003$	$0.939 \pm 0.009$
$f_2$ [–]	$0.995 \pm 0.004$	$1.029 \pm 0.007$	$0.994 \pm 0.002$	$0.942 \pm 0.006$
$b_1$ [%]	$-9.0 \pm 1.9$	$-15.2 \pm 0.2$	$0.4 \pm 1.0$	$4.5 \pm 0.4$
$b_2$ [%]	$2.1 \pm 1.2$	$-14.1 \pm 0.2$	$0.7 \pm 0.8$	$3.0 \pm 0.3$

[Title Page](#)

[Abstract](#)

[Introduction](#)

[Conclusions](#)

[References](#)

[Tables](#)

[Figures](#)

◀

▶

◀

▶

[Back](#)

[Close](#)

[Full Screen / Esc](#)

[Printer-friendly Version](#)

[Interactive Discussion](#)

Characterisation of  
water vapour isotope  
measurements by  
laser spectroscopy

F. Aemisegger et al.

**Table 5.** Standard deviation of laser spectroscopic isotope measurements at 5000 ppmv and 20 000 ppmv water vapour mixing ratio.

Instrument	$\delta^2\text{H}$ [% $\text{o}$ ]		$\delta^{18}\text{O}$ [% $\text{o}$ ]	
	at 5000 ppmv	at 20 000 ppmv	at 5000 ppmv	at 20 000 ppmv
L1115-i	1.3	0.6	0.22	0.25
L2130-i	1.1	0.4	0.25	0.19
WVIA	1.2	0.6	0.38	0.22

Title Page

Abstract

Introduction

Conclusions

References

Tables

Figures

|◀

▶|

◀

▶

Back

Close

Full Screen / Esc

Printer-friendly Version

Interactive Discussion



## Characterisation of water vapour isotope measurements by laser spectroscopy

F. Aemisegger et al.

**Table 6.** Key characteristics of the short-term stability of laser spectroscopic isotope measurements.  $\sigma_A$  is the Allan deviation.  $\tau_0$  is the optimal integration time.

Instrument	L1115-i		L2130-i		WVIA		WVIA-EP	
	$\delta^2\text{H}$	$\delta^{18}\text{O}$	$\delta^2\text{H}$	$\delta^{18}\text{O}$	$\delta^2\text{H}$	$\delta^{18}\text{O}$	$\delta^2\text{H}$	$\delta^{18}\text{O}$
$\tau_0$ [min]	15	30	80	80	10	7	30	60
$\sigma_A^{\tau_0}$ [%]	0.05	0.01	0.02	0.008	0.05	0.03	0.03	0.015
$\sigma_A^{5\text{s}}$ [%]	0.60	0.18	0.40	0.10	0.45	0.18	0.50	0.18

Title Page	
Abstract	Introduction
Conclusions	References
Tables	Figures
	
	
Back	Close
Full Screen / Esc	

Printer-friendly Version

Interactive Discussion

## Characterisation of water vapour isotope measurements by laser spectroscopy

F. Aemisegger et al.

**Table 7.** Average response times in s and corresponding standard deviations for the L1115-i and the WVIA instrument and the different water isotopic species. In total 103 switching experiments were performed, 54 switches to higher water concentrations (switch up,  $\tau_{\text{up}}$ ) and 49 switches to lower concentrations (switch down,  $\tau_{\text{down}}$ ).

	Picarro		WVIA	
	$\tau_{\text{up}}$ [s]	$\tau_{\text{down}}$ [s]	$\tau_{\text{up}}$ [s]	$\tau_{\text{down}}$ [s]
$\delta^2\text{H}$	29±3	43±4	3.3±0.3	5.7±2.5
$\delta^{18}\text{O}$	20±3	30±3	2.0±0.3	4.1±2.5
$\text{H}_2\text{O}$	15±2	16±3	2.5±0.2	3.3±2.1

<a href="#">Title Page</a>	<a href="#">Abstract</a>	<a href="#">Introduction</a>
<a href="#">Conclusions</a>	<a href="#">References</a>	
<a href="#">Tables</a>	<a href="#">Figures</a>	
<a href="#">◀</a>	<a href="#">▶</a>	
<a href="#">◀</a>	<a href="#">▶</a>	
<a href="#">Back</a>	<a href="#">Close</a>	
<a href="#">Full Screen / Esc</a>		

<a href="#">Printer-friendly Version</a>
<a href="#">Interactive Discussion</a>

## Characterisation of water vapour isotope measurements by laser spectroscopy

F. Aemisegger et al.

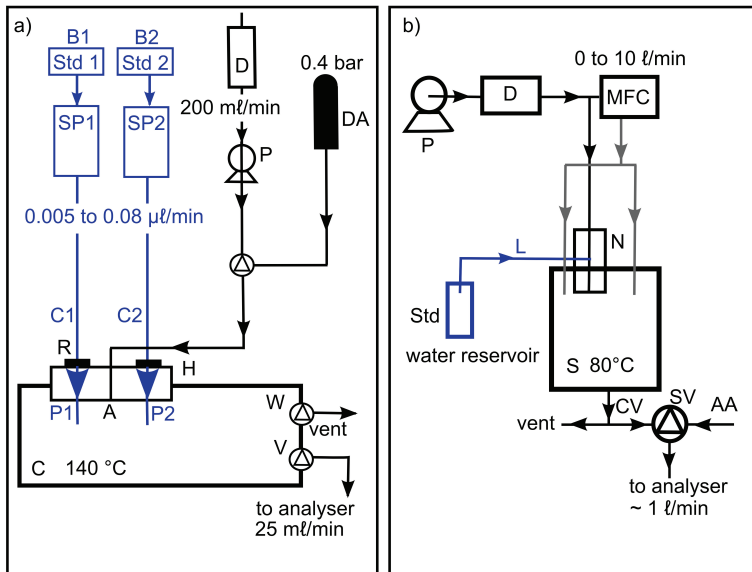


**Fig. 1.** Flow diagram of the calibration units. **(a)** Standard delivery module (SDM) by Picarro. Std1, Std2: liquid water standards; B1, B2: two collapsible bags for the standards; SP1, SP2: syringe pumps; C1, C2: capillary lines; P1, P2: needle ports; C vaporisation chamber; A: carrier gas inlet; H: injection head; R: o-rings; P: ambient air pump; D: molecular sieve 5 Å 200 cm<sup>3</sup> with Drierite indicator (Agilent) to dry ambient air as a carrier gas; DA: alternative carrier gas, dry synthetic air (Alphagases, Carbagas); W: waste port of the vaporisation chamber; V: outlet valve leading the calibration air to the measurement cell of the laser instrument. **(b)** The WVISS by LGR. Std: liquid water standard; L: capillary line; N: nebulising system; S: spray chamber; P: ambient air pump; D: drying system containing a regenerative desiccant air dryer and a replaceable Drierite cartridge; MFC mass flow controller for regulating carrier gas flow rate; SV: three way solenoid valve controlling the vapour source; CV: calibration vapour; AA: ambient air.

## Characterisation of water vapour isotope measurements by laser spectroscopy

F. Aemisegger et al.

**Fig. 2.** Example of a response to a step change in  $\delta^2\text{H}$  as measured by the L1115-i instrument. The total system response time consists of a time lag  $\tau_{\text{lag}}$ , which depends on the tubing length and pumping rate and an exponential time constant  $\tau_{\text{ads}}$  characterising the measured change in concentration from  $C_0$  to  $C_1$ , determined by the cavity gas exchange rate and the adsorption-desorption equilibrium on the tubing and cavity walls. The dashed lines delimit the data used for computing the concentration after the switch  $C_1$ . The black dashed dotted line indicates the switch time of the valve, the black full line indicates the instant when the vapour front of the new sample arrives in the cavity.

## Title Page

## Abstract

## Introduction

## Conclusion

## References

## Tables

## Figures

1

1

1

1

Bac

Close

Full Screen / Esc

Printer-friendly Version

## Interactive Discussion

## Characterisation of water vapour isotope measurements by laser spectroscopy

F. Aemisegger et al.

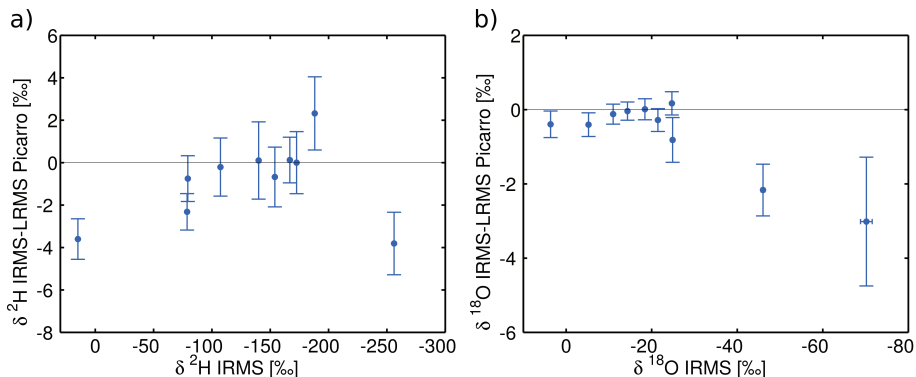


**Fig. 3.** Difference between L1115-i (LRMS Picarro, vertical axis) and IRMS for (a)  $\delta^2\text{H}$  and (b)  $\delta^{18}\text{O}$  isotope measurements for the ten WS 1–10 (Table 2).

[Title Page](#)[Abstract](#)[Introduction](#)[Conclusions](#)[References](#)[Tables](#)[Figures](#)[◀](#)[▶](#)[◀](#)[▶](#)[Back](#)[Close](#)[Full Screen / Esc](#)[Printer-friendly Version](#)[Interactive Discussion](#)

## Characterisation of water vapour isotope measurements by laser spectroscopy

F. Aemisegger et al.

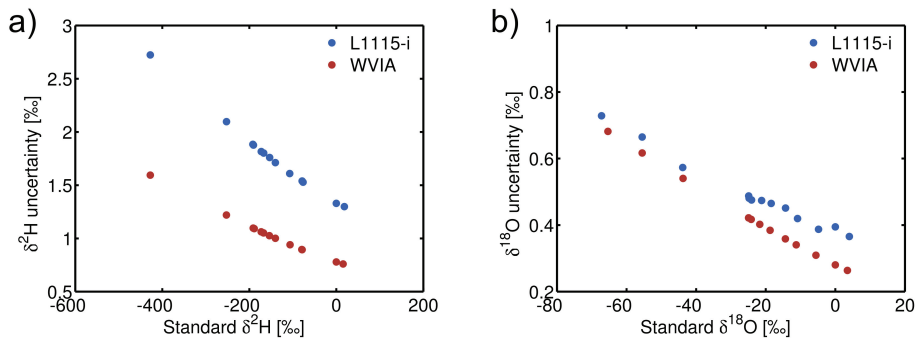


**Fig. 4.** Uncertainty of (a)  $\delta^2\text{H}$  and (b)  $\delta^{18}\text{O}$  isotope calibration runs by L1115-i and WVIA as a function of isotopic composition of the WS 1–10 as well as the IAEA standards (Table 2).

- [Title Page](#)
- [Abstract](#) [Introduction](#)
- [Conclusions](#) [References](#)
- [Tables](#) [Figures](#)
- [◀](#) [▶](#)
- [◀](#) [▶](#)
- [Back](#) [Close](#)
- [Full Screen / Esc](#)

[Printer-friendly Version](#)[Interactive Discussion](#)

## Characterisation of water vapour isotope measurements by laser spectroscopy

F. Aemisegger et al.

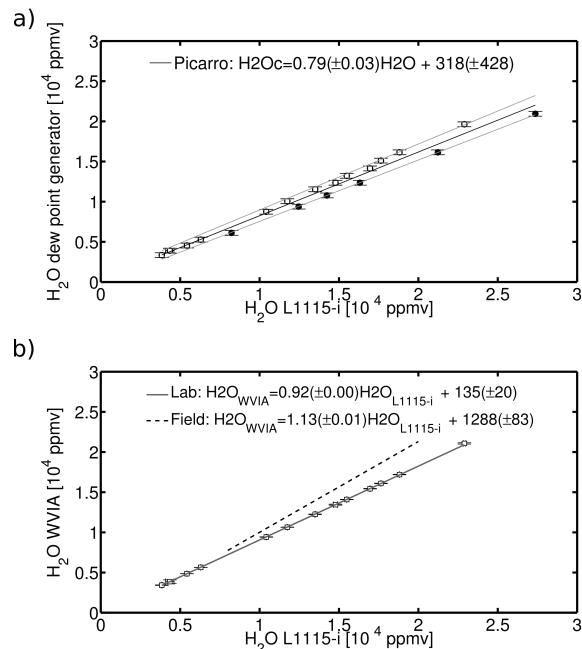


**Fig. 5.** Calibration of water vapour mixing ratio measurements. **(a)** L1115-i laboratory calibration measurements. The calibration experiment with the dew point generator was done twice; once with L1115-i connected to the LI-610 alone (full circles) and once with L1115-i and WVIA connected in parallel to the LI-610 (open squares). A least squares fit to all data points of the two experiments is shown by the black line. The grey lines show the standard deviation of the least square fit. In **(b)** WVIA and L1115-i measurements are compared using parallel laboratory measurements (grey line) and parallel field measurements (black dashed line). The laboratory data points (black squares) show average measured water concentration of hourly runs and their standard deviation. The grey line represents a least square fit to the laboratory data points. The black dashed line represents the least square fit to the ambient air measurements. The uncertainty of these fits is very small and thus not shown.

[Title Page](#)

[Abstract](#)

[Introduction](#)

[Conclusions](#)

[References](#)

[Tables](#)

[Figures](#)

[◀](#)

[▶](#)

[Back](#)

[Close](#)

[Full Screen / Esc](#)

[Printer-friendly Version](#)

[Interactive Discussion](#)

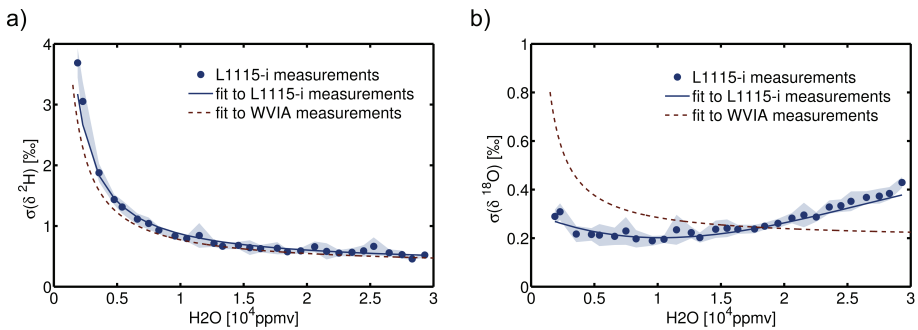


**Fig. 6.** Dependency of the  $\delta^2\text{H}$  (a) and  $\delta^{18}\text{O}$  (b) measurement precision (average standard deviation  $\sigma$  of calibration runs) on water vapour mixing ratio for L1115-i (solid lines and data points). The fit to the WVIA measurements (dashed lines) found by Sturm and Knohl (2010) is shown for comparison. The shading represents the standard deviation of all calibration runs with four different standards (WS 6–9 in Table 2).

F. Aemisegger et al.

## Title Page

## Abstract

## Introduction

## Conclusion:

## References

## Tables

## Figures

1

A small white play button icon with a triangle pointing right and a vertical bar to its right, located in the bottom right corner of the slide.

Bac

Close

Full Screen / Esc

5

## Interactive Discussion

## Characterisation of water vapour isotope measurements by laser spectroscopy

F. Aemisegger et al.

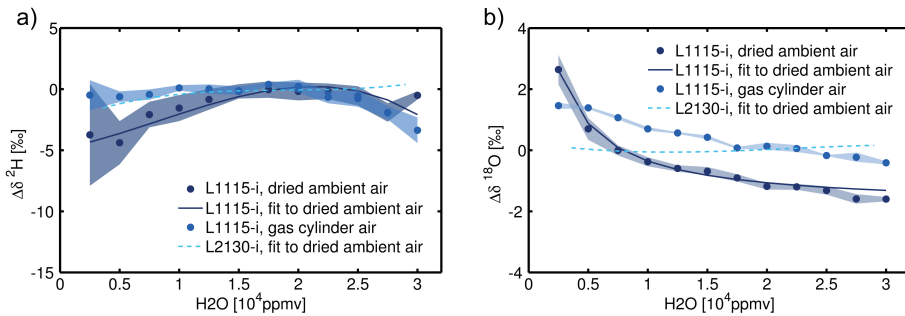


**Fig. 7.** Dependency of the L1115-i isotope measurements on water vapour mixing ratio for  $\delta^2\text{H}$  in **(a)** and  $\delta^{18}\text{O}$  in **(b)**. The data was calibrated independently using the WVISS calibration unit and the IAEA standards VSMOW2 and SLAP2 at a water vapour mixing ratio of 18 000 ppmv. The shading represents the standard deviation of all calibration runs with four different working standards (WS 6–9 in Table 2). The full black curves are least square fits to the data obtained using dried ambient air as a carrier gas. The dashed curves show least square 3rd order polynomial fits to the L2130-i measurements.

- [Title Page](#)
- [Abstract](#) [Introduction](#)
- [Conclusions](#) [References](#)
- [Tables](#) [Figures](#)
- [◀](#) [▶](#)
- [◀](#) [▶](#)
- [Back](#) [Close](#)
- [Full Screen / Esc](#)

- [Printer-friendly Version](#)
- [Interactive Discussion](#)

## Characterisation of water vapour isotope measurements by laser spectroscopy

F. Aemisegger et al.

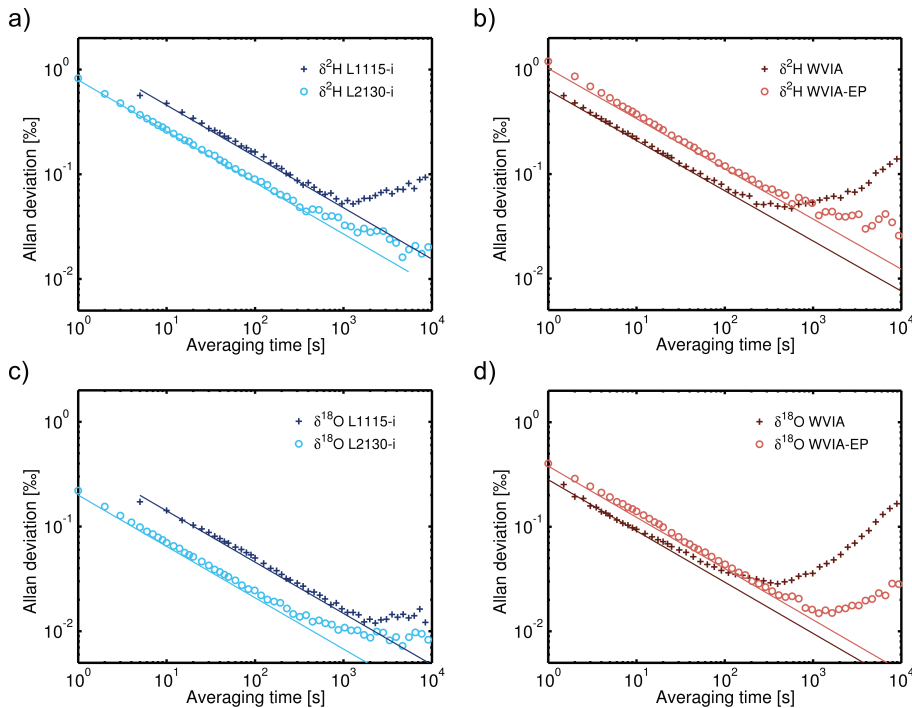


**Fig. 8.** Short-term stability of  $\delta^2\text{H}$  (a and b) and  $\delta^{18}\text{O}$  measurements (c and d) at 15 700 ppmv water vapour mixing ratio by L1115-i/L2130-i (a and c) and WVIA/WVIA-EP (b and d). The square root of the Allan variance is shown as a function of aggregation time on a log-log scale. The solid lines show the expected behaviour of a pure white noise signal with the same variance as the measured signal at the time scale of data acquisition (5 s for L1115-i and 1 s for WVIA, WVIA-EP, L2130-i).

[Title Page](#) [Abstract](#) [Introduction](#)  
[Conclusions](#) [References](#) [Tables](#) [Figures](#)  
[◀](#) [▶](#) [◀](#) [▶](#)  
[Back](#) [Close](#) [Full Screen / Esc](#)

[Printer-friendly Version](#)  
[Interactive Discussion](#)

## Characterisation of water vapour isotope measurements by laser spectroscopy

F. Aemisegger et al.

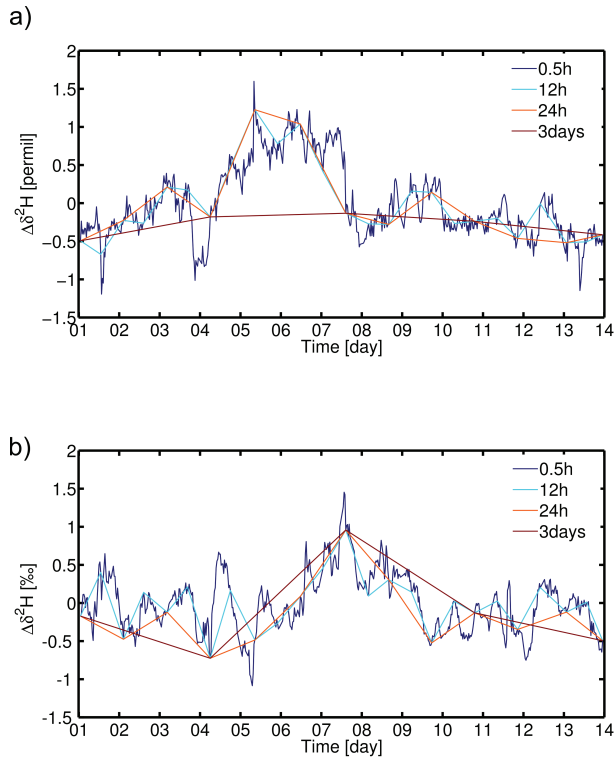


**Fig. 9.** Temporal evolution of the bias correction amplitude of isotope measurements with L1115-i **(a)** and WVIA **(b)** at 15 700 ppmv water vapour mixing ratio over 14 days. Each line corresponds to one calibration frequency scheme. The dark blue correction curve is obtained if the instrument is calibrated every 30 min.

## Title Page

## Abstract

## Introduction

## Conclusion

## References

## Tables

## Figures

14

1

Back

Close

Full Screen / Esc

[Printer-friendly Version](#)

## Interactive Discussion

**Characterisation of water vapour isotope measurements by laser spectroscopy**

F. Aemisegger et al.

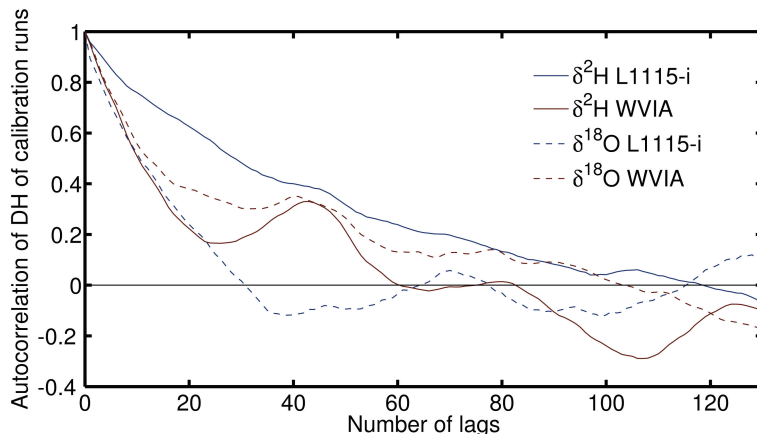


**Fig. 10.** Autocorrelation function of the isotopic composition of the calibration runs of the long term stability experiment for L1115-i and WVIA. A lag of 1 corresponds to a 30 min calibration interval.

[Title Page](#)[Abstract](#)[Introduction](#)[Conclusions](#)[References](#)[Tables](#)[Figures](#)[◀](#)[▶](#)[◀](#)[▶](#)[Back](#)[Close](#)[Full Screen / Esc](#)[Printer-friendly Version](#)[Interactive Discussion](#)

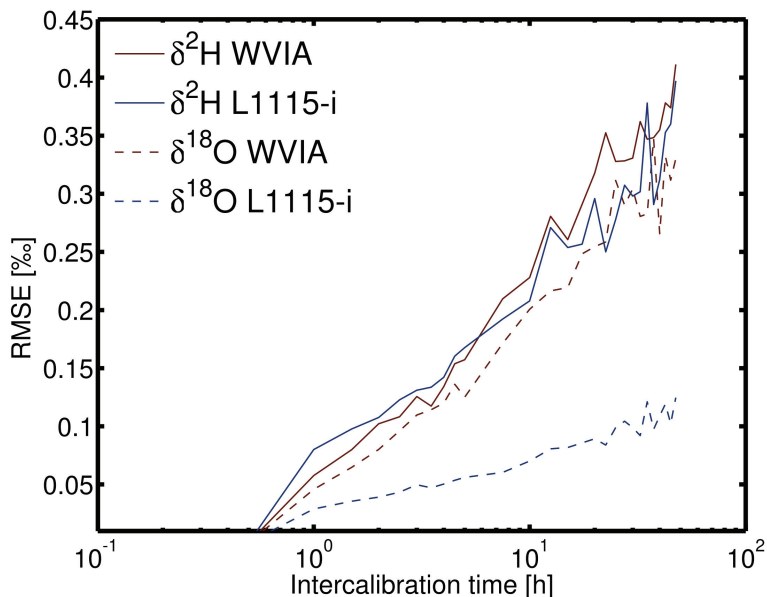


**Fig. 11.** Root mean square error (RMSE) of laser spectroscopic isotope measurements as a function of intercalibration time on a log scale.

## Characterisation of water vapour isotope measurements by laser spectroscopy

F. Aemisegger et al.

## Title Page

## Abstract

## Introduction

## Conclusion

## References

## Tables

## Figures

1

1

1

Bac

Close

Full Screen / Esc

10 of 10

## Interactive Discussion

**Characterisation of water vapour isotope measurements by laser spectroscopy**

F. Aemisegger et al.

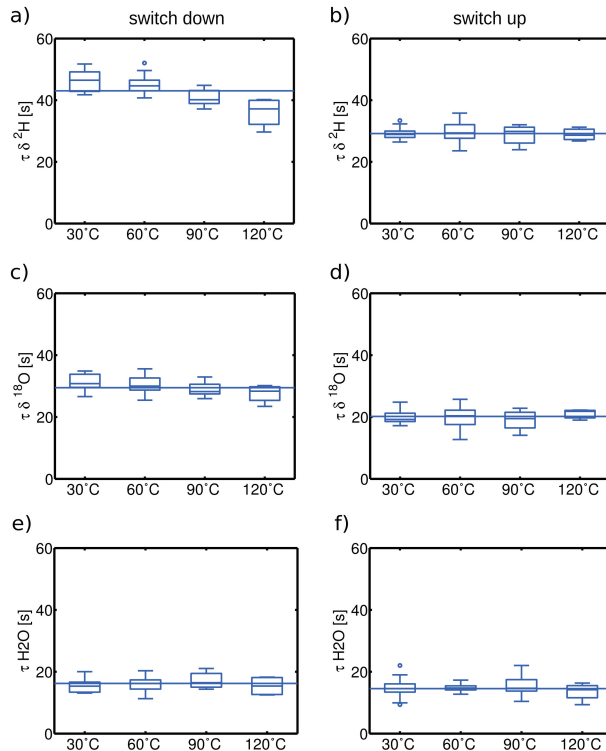


**Fig. 12.** Typical response times  $\tau_{\text{ads}}$  for the L1115-i isotope measurements. The boxplots show the distribution of response times as a function of tubing temperature. The left column of plots show switches to lower water vapour mixing ratios (switch down) and the right column of plots shows switches to higher water vapour mixing ratios (switch up).

## Characterisation of water vapour isotope measurements by laser spectroscopy

F. Aemisegger et al.

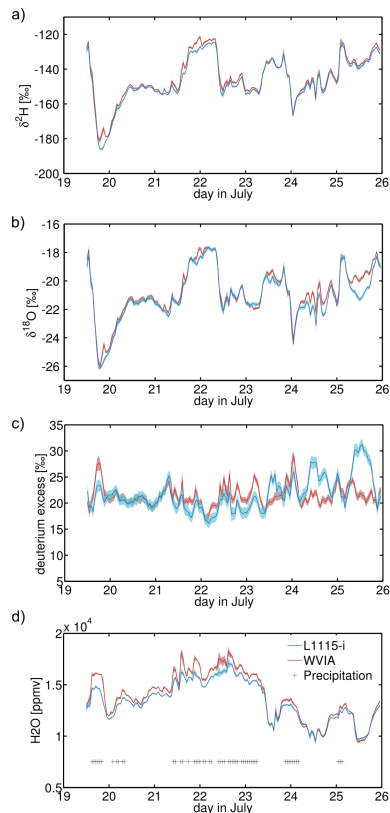


**Fig. 13.** Time series of  $\delta^2\text{H}$  (a),  $\delta^{18}\text{O}$  (b), deuterium excess (c) and water vapour mixing ratio (d) from ambient air measurements in Zurich from 19–26 July 2011 with L1115-i in blue and WVIA in red. The data is averaged to 1 h and the shaded area shows the 1 h standard deviation based on 5 s measured data for L1115-i and 5 s averaged data for WVIA. Crosses in (d) indicate the occurrence of precipitation.

## Characterisation of water vapour isotope measurements by laser spectroscopy

F. Aemisegger et al.

## Title Page

## Abstract

## Introduction

## Conclusions

## References

## Tables

## Figures

1

1

Back

Close

Full Screen / Esc

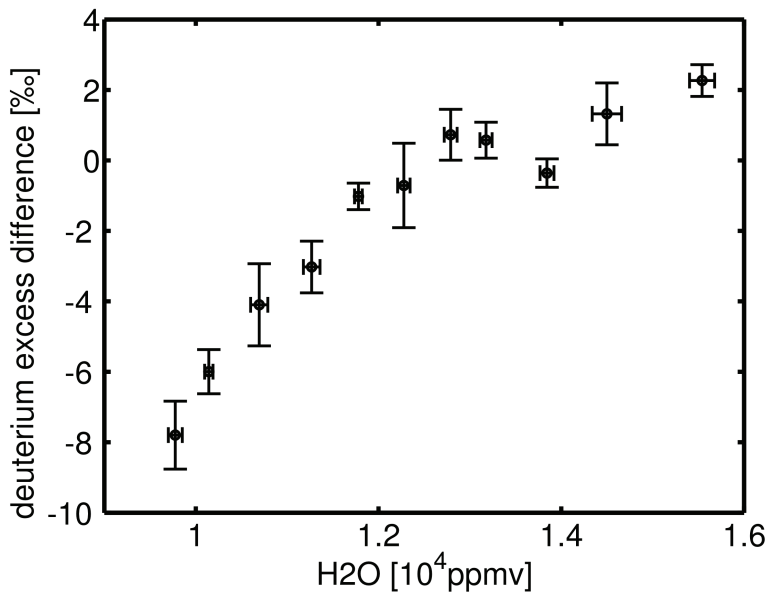


**Fig. 14.** Dependency of the deuterium excess difference between L1115-i and WVIA on the ambient water vapour mixing ratio during the comparative field measurement on the roof of a tower building in Zurich from 19–26 July 2011.